Title
Voltage- and Calcium-Activated Potassium Channel Voltage Sensor Remodeling by Modulatory Beta Subunits and Heme

Author
Park, Saemi

Publication Date
2014

Peer reviewed|Thesis/dissertation

UNIVERSITY OF CALIFORNIA

Los Angeles

Voltage- and Calcium-Activated Potassium Channel Voltage Sensor Remodeling by Modulatory Beta Subunits and Heme

A thesis submitted in partial satisfaction

of the requirements for the degree Master of Science

in Physiological Sciences

by

Saemi Park

2014

ABSTRACT OF THE THESIS

Voltage- and Calcium-Activated Potassium Channel Voltage Sensor Remodeling by Modulatory Beta Subunits and Heme

by

Saemi Park

Master of Science in Physiological Sciences

University of California, Los Angeles, 2014

Professor Alan Grinnell, Co-Chair

Professor Riccardo Olcese, Co-Chair

Large-conductance voltage- and Ca^{2+}-activated K^{+} channels (BK) have a broad distribution of expression in mammalian cells. BK channels are activated by the membrane depolarization and elevation of intracellular free calcium. When the channel is activated, it allows an increase in potassium permeability, which hyperpolarizes the membrane electrical potential, suppressing cellular excitability. This membrane hyperpolarization decreases the activity of voltage-gated channels, including Ca^{2+} channels: the latter confers a significant role of BK channels in the internal calcium homeostasis. BK channels are involved in various fundamental physiological

processes including the control of blood pressure and neuronal excitability. The BK channel is a homotetramer consisting of four pore-forming alpha subunits, which encode for seven membrane-spanning domains (S0-S6) and two large intracellular domains, RCK1 and RCK2. S0-S4 segments are known as the voltage sensing domain (VSD); S5 and S6 form the pore region and are involved in ion selectivity, while the RCK domains assemble into the ligand-sensing Gating Ring superstructure. In different tissues, the activity of BK alpha subunits is tuned by their association with modulatory beta subunits, beta1-4. The first project investigated the voltage-dependent structural rearrangements of the human BK channel in the presence of beta1 subunit. The data showed that the association of beta 1 remodeled the VSD movements. It is postulated that the association with beta1 destabilizes the active conformation of the voltage sensor in the absence of Ca^{2+}, thus producing an overall right shift in its voltage dependence. BK channels are also modulated by small cytosolic ligands such as heme. The RCK1-RCK2 linker possesses a conserved heme regulation motif (HRM) and exhibited structural homology to cytochrome C (CytC), a hemoprotein. In particular, BK Methionine-691 aligned with M80 of the CytC, the second axial ligand (outside the HRM) to the heme iron. The goal of the second project aimed to understand the role of M691 in the BK regulation by heme. The mutation M691A dramatically diminished the inhibition of BK channel opening by heme (100 nM) compared with the wild-type BK, suggesting that M691 is critical for heme binding.

The thesis of Saemi Park is approved.

Gordon Fain

Alan Grinnell, Committee Co-Chair

Riccardo Olcese, Committee Co-Chair

University of California, Los Angeles

2014

DEDICATION

This thesis is dedicated to my Korean and American parents whose sacrifice allowed me to pursue my dreams. I would also like to dedicate my thesis to my best friend and boyfriend, Hak Jo Kim, whose support helped me finish the Master's degree. Lastly, I would like to dedicate my work to my sister Sumin for her never ending encouragement.

TABLE OF CONTENTS

LIST OF FIGURES

ACKNOWLEDGEMENTS

I would like to thank my mentor and committee chair, Dr. Riccardo Olcese, for his wonderful guidance throughout the graduate program at UCLA and helping me pursue my passion in research. Also, I want to thank my committee members, Drs. Alan Grinnell and Gordon Fain for their great support. This thesis project would not be successful without help and expertise from Drs. Antonios Pantazis, Nicoletta Savalli, and Taleh Yusifov. I have been blessed with RO lab members as well as great classmates in the Integrative Biology and Physiology Department.

CHAPTER 1: INTRODUCTION

Ion Channels

Ion channels are transmembrane proteins that serve as macromolecular pores to permit the flux of ions (Hille, 2001). Pores of most ion channel proteins across the membrane of animal cells are narrow and highly selective (Alberts *et al.*, 2002). Ion channels have an efficient ion transport rate, 10^5 times faster than the maximum rate of transport of the any carrier protein (Alberts *et al.*, 2002). Because ion channels do not use an energy source to transport actively, the mediated transport is down electrochemical gradients (Alberts *et al.*, 2002). Inorganic ions such as Na^+, K^+, Ca^{2+}, or Cl^- diffuse through ion channels across the lipid bilayer membrane (Alberts *et al.*, 2002). In various cells, the mediation of ion fluxes via channels contributes to fundamental functions (Alberts *et al.*, 2002), which include setting the resting membrane potential, shaping electrical signals, regulating the movement of messenger Ca^{2+}, and modulating the net ion flux across the epithelial cells of secretory tissues (Hille, 2001).

Ion channels can open and close in response to different stimuli (Hille, 2001). To be specific, different stimuli that can promote channel opening include changes in membrane potential, temperature, mechanical stress, and ligand binding (Cui *et al.*, 2009; Hou *et al.*, 2009; Latorre *et al.*, 2010; Lee & Cui, 2010). The major types of ion channels based on their activation mechanism are voltage- and ligand-gated channels (Hille, 1992). Voltage-gated ion channels open and close by sensing changes in the membrane potential with voltage sensor domains (Bezanilla, 2008; Swartz, 2008). In most cases, two states of voltage sensors include resting and active states in order to operate the opening of the channel (Swartz, 2008). Voltage-gated ion channels have low channel open probability when the voltage sensors are in the resting state;

membrane depolarization can promote voltage sensor activation and in turn increase the channel open probability (Lehmann-Horn & Jurkat-Rott, 1999). The mechanism of voltage sensing is discussed in the later section.

Ligand-gated ion channels conduct ions across cell membranes in response to extracellular neurotransmitters including acetylcholine, glutamate, glycine, or gamma-aminobutyric acid (Hille, 1992; Swartz, 2008). Also, binding of intracellular mediators such as ions or nucleotides can cause the channel to open by inducing a conformational change of the channel (Alberts *et al.*, 2002). For example, the increased concentration of cyclic guanosine monophosphate (cGMP) in darkness promotes the open state of channels in the rod plasma membrane to allow the flux of cations such as Na^+ and Ca^{2+} (Fain, 2011). Also, the binding of intracellular Ca activates BK channels (Wei *et al.*, 1994).

Ion Selectivity and Gating

Two critical properties of ion channels include ion selectivity and gating. The channel contains the narrowest part of the passage called the selectivity filter, which limits passage for the permeating ions with associated water molecules. Therefore, a high concentration of ions increases the ion flux through the channel but only up to the maximum rate. As one of the properties of ion channels, gating of the channels separates them from any simple aqueous pores. Ion channels fluctuate between open and closed states in response to certain stimuli, discussed in the previous section. The prolonged stimulation by depolarization or ligand binding promotes some ion channels to enter non-conducting inactive or desensitized states, respectively, which makes them resistant to channel opening (Alberts *et al.*, 2002).

The BK Channel

Large-conductance voltage- and Ca^{2+}-activated K^+ channels (BK) are unique in that they are gated by both voltage and ligands, and they have a broad distribution in mammalian cells (Hoshi *et al.*, 2013; Latorre & Brauchi, 2006; Latorre *et al.*, 2010). BK channels are activated by membrane depolarization and elevation of intracellular free calcium concentration ($[Ca^{2+}]_i$), conferring a significant role in the regulation of membrane excitability and internal calcium homeostasis (Shipston, 2013). Because of their exquisite Ca sensitivity, Yazejian *et al*. (2000) showed that endogenous BK channels can be used to measure the dynamics of intracellular Ca^{2+} changes at active zones of the *Xenopus* nerve terminal during synaptic activity. BK channels are involved in various basic physiological processes including the control of blood flow and neuronal excitability (Shipston, 2013). For instance, in vascular smooth muscle, BK channel activation by membrane depolarization and $[Ca^{2+}]_i$ elevation leads to K^+ efflux and thus induces membrane hyperpolarization, which in turn deactivates voltage-gated Ca^{2+} channels (Ledoux *et al.*, 2006). Thus, intracellular calcium concentration decreases and the muscle relaxes. Therefore, BK channels play an important role in setting vascular tone (Ledoux *et al.*, 2006). Also, BK channels are involved in the regulation of the circadian rhythm (Meredith *et al.*, 2006). In the suprachiasmatic nucleus (SCN), BK channels play a major role in repolarization of the membrane after an action potential (Colwell, 2011). In order to have day and night difference in the circadian rhythm of the SCN neurons, K^+ conductance is inactive during the day and active at night (Kuhlman and McMahon, 2004; Kuhlman and McMahon, 2006). Although it is not clear what mechanism is driving the day and night difference in circadian rhythms of SCN neurons to date, recent work has shown that BK channels are partially responsible for silencing electrical

activity at night by hyperpolarizing the cell membrane (Montgomery & Meredith, 2012; Montgomery *et al.*, 2013). Dysfunction of BK channels may lead to numerous pathophysiological conditions, including hypertension (Grimm & Sansom, 2010), asthma (Seibold *et al.*, 2008), epilepsy and dyskinesia (Du *et al.*, 2005).

BK Channel Membrane Topology and Structure

The BK channel pore-forming alpha subunit contains seven membrane-spanning domains (S0-S6) as shown in Figure 1A (Meera et al., 1997; Wallner et al., 1996). S1-S6 segments are homologous to regions of proteins of the voltage-gated potassium channel (K_V) family, but BK channels in particular have an additional unique transmembrane helix (S0), which brings the N-terminus extracellular (Wallner *et al.*, 1996). S0-S4 segments are known as the voltage sensing domain (VSD) while S5 and S6 form the pore region and are involved in ion selectivity (Latorre & Brauchi, 2006). The transmembrane region is only about a third of the entire amino-acid residues and the rest is the cytoplasmembrane domain (C-terminus) (Hoshi *et al.*, 2013). This cytoplasmic C-terminal domain consists of two regulators of conductance for K^+ (RCK1 and RCK2) (Hoshi *et al.*, 2013). The transmembrane segment S6 and RCK1 are linked by a short stretch of amino-acids (~20 residues), and a long loop (~ 100 residues) connects RCK1 and RCK2 (Hoshi *et al.*, 2013). The BK C terminus encompasses two Ca^{2+} sensors with micromolar affinity: one in RCK1 (Xia *et al.*, 2002;Yusifov *et al.*, 2010) and one in RCK2 (Yusifov et al., 2008), known as the "Ca bowl" (Schreiber & Salkoff, 1997). A large cytoplasmic structure, the "Gating Ring" (GR) (Fig 1B), is formed by the assembly of four pairs of RCK1-RCK2 domains in the homotetrameric BK channel (Leonetti *et al.*, 2012; Yuan *et al.*, 2010; Wu *et al.*, 2010) and is responsible for transducing ligand sensitivity to the pore (Javaherian *et al.*, 2011; Savalli *et al.*,

2012; Miranda *et al.*, 2013; Budelli *et al.*, 2013). The functional interactions between the transmembrane and Gating Ring domains are allowed because of their close proximity (Yang *et al.*, 2008) although the exact distance is not known yet.

The Voltage-Sensing Domain

The plasma membrane of cells separates the cytoplasm from the external medium. Different ionic species keep their concentration in equilibrium across the bilayer depending on their electrochemical gradient (Bezanilla, 2008; Swartz, 2008). Due to the distribution of these ionic species, different charges exist across the membrane, which is converted to a membrane potential between ~-40mV and ~–100 mV (negative inside the cell). The membrane potential can vary based on the cell type and the cell cycle phase. In response to changes in the membrane potential, an electric charge or an electric dipole can be re-adjusted in a different way within a transmembrane protein, causing a protein conformational change that may control its function (Bezanilla, 2008). A measurable transient/gating current is increased by the movement of the charge or dipole (Armstrong & Bezanilla, 1973). There are different mechanisms to sensing the electric field in proteins (Fig 2). The possible candidates are charged amino acids such as Asp, Glu, Arg, Lys and His because of their ability to orient in the field and traverse it (Fig 2A). On the other hand, the voltage can be sensed by amino acid side chains with an intrinsic dipole moment such as Tyr (Fig 2B). As another alternative, the α-helix with its intrinsic dipole moment constitutes a possible voltage-sensing structure (Fig 2C). Also, free ions can associate in the cavities of proteins. The protein changes its conformation as a result of the movement of the free ions promoted by changes in an electric field (Fig 2D) (Bezanilla, 2008).

The voltage-sensing domain (VSD) is formed by the conserved S1–S4 transmembrane segments of voltage-activated ion channels. The fourth membrane-spanning segment, S4, is notable as it contains several positively charged residues (Arg or Lys) (Noda *et al.*, 1986; Tempel *et al.*, 1987). Charged residues may also be carried in S1–S3 segments. Despite the original thought that only voltage-activated ion channels contain S1–S4 voltage-sensing domains, it has been shown that a VSD contributes to the regulation of the hydrolysis of membrane phosphoinositides in a phosphatase from the *Ciona intestinalis* (Fig 3) (Murata *et al.*, 2005; Kohout *et al.*, 2008). Another exception is the voltage-activated proton channel which consists of the S1–S4 segments without a distinct pore domain (Fig 3) (Sasaki et al., 2006; Ramsey et al., 2006). The information about the three-dimensional distribution of S1–S4 domains with respect to the pore was obtained from the X-ray structures of the bacterial K_VAP and the eukaryotic K_V1.2 channel: the VSD adopts transmembrane orientation and seems to have a loose attachment to the pore domain (Jiang *et al.*, 2003; Long *et al*., 2005; Long *et al.*, 2007).

In the BK channel, the VSD is composed of conserved transmembrane helices S1-S4 with the S0 segment. Based on electrophysiological studies, overall 2.4 charges were estimated per BK channel (Diaz *et al.*, 1998; Horrigan & Aldrich, 1999; Horrigan *et al*., 1999), notably less than a typical K_V channel (up to ~16 charges per channel (Jensen *et al.*, 2012). Typically, the S4 segment of the BK channel carries four positively-charged Arg residues (R0, R2, R3, and R4 equivalent to K_V channels) (Fig 4); but only R4 contributes to voltage sensing (Ma *et al.*, 2006; Pantazis *et al.*, 2010a). Another example of different characteristics from a typical K_V channel is that the S2 and S3 of the BK VSD contains charged amino acids that play a critical role in sensing the voltage (Ma *et al*., 2006; Pantazis *et al.*, 2010a); thus the BK channel carries fewer

and more "decentralized" voltage-sensing charges than in K_V channels (Fig 4). To be specific, S2 bears two voltage-sensing residues, Asp135 and Arg167, and S3 has an additional voltage-sensing charge, Asp186 (Ma *et al.*, 2006). This charge distribution leads to complex relative motions during voltage-dependent activation: fluorometry experiments propose that S4 diverges from S0, S1 and S2, while S2 approaches S1 upon depolarization of the membrane (Pantazis & Olcese, 2012; Pantazis et al., 2010b). The voltage-dependent movements of S2 and S4 segments reciprocally enhance their voltage-sensing properties in a collaborative mode (Pantazis *et al.*, 2010a). In agreement with the idea that the BK voltage-sensing process involves multiple voltage-sensing charges at different positions, multiple kinetic components can appear in BK gating currents (Contreras *et al.*, 2012).

How do voltage-dependent VSD movements open the channel pore? In K_V channels, the S4-S5 linker seems to function as a linkage mechanism connecting the movement of VSD to open the ion conduction gate at the cytoplasmic ends of the four S6 segments (Long *et al.*, 2007; Jensen *et al.*, 2012). However, the structural correlates of the BK VSD-gate coupling mechanism are not clear. It is possible that the S6-RCK1 linker, connecting the transmembrane region of the protein with the Gating Ring domain, has a role in the VSD-gate coupling process. The length of this linker segment in the absence of Ca^{2+} changes the open-state probability and voltage curve position on the voltage axis without a major difference in steepness of the curve (Niu *et al.*, 2004). In addition, it has been suggested that Leu and Phe residues positioned in the middle of S6 mediates the effects of VSD activation and Ca^{2+} binding on the ion conduction gate equilibrium (Wu et al., 2009).

Voltage and Calcium Dependency

BK channels open in response to both voltage and the intracellular calcium, and their voltage dependence varies depending on the calcium concentration (Horrigan & Aldrich, 2002; Latorre *et al.*, 2010; Hoshi *et al.*, 2013). The increase of intracellular calcium concentration can shift the conductance-voltage curves towards more hyperpolarized potentials, producing channel opening at more negative potentials (Fig 5). When the ion conduction gate is closed, the BK VSD is stabilized in the resting conformation in the absence of intracellular Ca^{2+}. Membrane depolarization activates the BK voltage sensors, which increases the pore open probability (P_O). When the ion conduction gate is open, the voltage sensors can be activated by depolarization more easily. Also, the Ca^{2+} affinity is increased by the activation of the voltage sensors, and binding Ca^{2+} further assists voltage-sensor activation. Thus, depolarization and/or greater intracellular calcium concentration promotes channel opening (Hoshi *et al.*, 2013).

Modulatory Subunits

BK channels co-assemble with auxiliary subunits beta1-4, and leucine-rich repeat-containing proteins (LRRCs; gamma subunits), allowing functional diversity by modulating Ca^{2+} and voltage sensitivity as well as their kinetic properties, and current inactivation and/or rectification (Wallner *et al.*, 1995; Jiang *et al.*, 1999; Yan & Aldrich, 2012). Studied in this thesis, BK beta subunits consist of two transmembrane (TM) helices, TM1 and TM2, connected by a long extracellular loop as shown in Fig.1A (Poulsen *et al.*, 2008; Sun *et al.*, 2012). Co-assembly of BK channels with beta1 subunits is abundant in arterial smooth muscle (Brenner *et al.*, 2000; Orio & Latorre, 2005; Wallner *et al.*, 1995). Beta1 subunits slow down BK channel activation and modify the voltage- and Ca^{2+}-sensing properties of BK channels. Beta2 subunits, expressed

mostly in the brain and endocrine cells, have a striking feature that allows BK channels to have fast inactivating properties by a "ball and chain"-like mechanism (Brenner *et al.*, 2000; Hu *et al.*, 2003; Orio & Latorre, 2005; Uebele *et al.*, 2000; Wallner *et al.*, 1999; Xia *et al.*, 1999). In testes and adrenal cells, beta3 subunits are abundant and inactivate the BK channel (Uebele *et al.*, 2000; Orio *et al.*, 2006; Wu *et al.*, 2013). Beta4 subunits are primarily expressed in the brain and reduce the sensitivity to changes in membrane potential (Contreras *et al.*, 2012).

Fig. 6 shows the differential modulation of BK channels by beta1 and beta2 subunits across a wide range of intracellular calcium concentration (Orio *et al.*, 2006). At high $[Ca^{2+}]_i$, both beta1 and beta 2 subunits facilitate BK channel opening at more negative membrane potentials (Orio *et al.*, 2006). However, BK channels co-expressed with beta1 do not show this left shift of the conductance-voltage relationship at submicromolar intracellular calcium concentrations (Orio *et al.*, 2006). Also, previous studies showed that the presence of beta2 subunits altered the voltage-sensing and kinetics properties of BK VSDs, mainly represented by S4 (Savalli *et al.*, 2007; Contreras *et al*., 2012). Moreover, the coexpression of beta2 enhances channel opening by facilitating voltage sensor activation (Savalli *et al.*, 2007).

Modulation of the BK Channel by Small Molecules

In addition to voltage and Ca^{2+}, BK channels are modulated by various small molecules including protons (H^+), heme/hemin, Mg^{2+}, carbon monoxide, reactive oxygen/nitrogen species, lipids, and metabolites (Latorre *et al.*, 2010; Cui *et al.*, 2009; Lee & Cui, 2010; Hou *et al.*, 2009). Hemin, the oxidized form of heme [Fe(II) protoporphyrin-IX], has been shown to decrease the opening of BK channels at depolarized membrane potentials (Horrigan *et al.*, 2005). It has been

shown that heme interacts with the linker region between RCK1 and RCK2 (Tang et al., 2003; Yi et al., 2010; Jaggar et al., 2005), which contains a conserved heme-binding motif (CXXCH) (Tang *et al.*, 2004; Wood & Vogeli, 1997) (Hou *et al.*, 2009). The sensitivity of the BK channel to heme was disrupted by mutations in this sequence (Williams *et al.*, 2004; Tang *et al.*, 2003; Jaggar *et al.*, 2005), suggesting that this sequence serves as the binding site for heme (Hou *et al.*, 2009). As an important regulator of protein function, heme has been shown to reduce the allosteric coupling of voltage sensor activation and Ca^{2+} binding to channel opening (Horrigan *et al.*, 2005).

Thesis Aims

Understanding the operation of BK channels is critical not only because they are involved in various physiological functions but also because their dysfunction can lead to detrimental pathophysiological conditions (Du et al., 2005; Werner et al., 2005; Seibold et al., 2008; Grimm & Sansom, 2010). Thus, gaining knowledge about the BK channel will tremendously contribute to the basis of the medical research related to BK dysfunction. In my Master's Thesis project, I studied the molecular bases of altered BK channel voltage sensitivity in the presence of beta1 subunits, in particular the structural rearrangement of the Voltage Sensor transmembrane segments in the absence or presence of beta1 subunits. In the second part of my thesis, I investigated the role of a methionine (M691) in the linker of RCK1 and RCK2 on heme-mediated BK channel regulation, which may act as a coordinating heme residue. To address these questions, I used two voltage clamp techniques: Cut-open Oocyte Vaseline Gap (COVG) voltage clamp fluorometry and patch clamp.

CHAPTER 2: Materials and Methods

Molecular biology

Mutagenesis: Single point mutations were generated with the QuikChange Site-Directed Mutagenesis Kit (Stratagene, CA). *In vitro* site-directed mutagenesis is a very useful tool to study the relationship between protein structure and function. The QuikChange site-directed mutagenesis method allows site-specific mutation in double-stranded plasmids. It is performed using PfuUltra™ high-fidelity DNA polymerase. The PCR product is checked on a 1% agarose gel and then transformed into competent bacteria, XL1-blue, with the appropriate selective antibiotics. The mutations were then confirmed by sequencing. A hSlo clone (#U11058) without extracellular cysteines (C14S-C141S-C277S) was used (Savalli et al., 2006). Background mutations also included R207Q to increase P_O at low $[Ca^{2+}]_i$ (Diaz et al., 1998; Ma et al., 2006). A single cysteine was substituted at position 135 for site directed fluorescence labeling in order to track voltage-dependent conformational rearrangements in the vicinity of the extracellular flank of the S1 transmembrane segment (Pantazis & Olcese, 2012).

In vitro transcription: The plasmids carrying cDNAs of WT and mutant channels were linearized with a specific single-cutter restriction enzyme (generally Not I, New England Bioloab). The linear cDNA was then used as the template for *in vitro* transcription (1-2 ug per reaction) to produce capped cRNAs (mMESSAGE MACHINE; Ambion, Austin, TX). Capped RNA mimics most eukaryotic mRNAs found *in vivo*, because of a 7-methyl guanosine cap structure at the 5' end. The reaction of the *in vitro* transcription kit includes the cap analog [m7G(5')ppp(5')G], which is incorporated as the first or 5' terminal G of the transcript because its structure precludes its incorporation at any other position in the RNA molecule. The reaction ran at 37^{o}C for 2h. The

cRNA was then precipitated with LiCl2 at 20^{o}C and resuspended in water. After assessing RNA concentration with the spectrophotometer (wavelength = 260 nm) and RNA quality by agarose gel, cRNA was stored at –80^{o}C.

Oocyte preparation and injection

Xenopus laevis (NASCO, Modesto, CA) oocytes are an excellent system to express ion channels for electrophysiological studies, as their large size (~1 mm diameter) allows the micro-injection of cloned RNA into their cytosol, which is readily translated into functional protein. After surgical excision from the frog, the oocytes (stage V-VI) were defolliculated via a mechanical and enzymatic treatment (collagenase type I in a Ca^{2+}-free solution). The same day of preparation or the day after, oocytes were injected with 50 nl of total cRNA (0.01-0.1 ug/ul) with a Drummond nano-injector. Injected oocytes were maintained at 18°C in an amphibian saline solution supplemented with 50 ug/ml gentamycin (Invitrogen, Carlsbad, CA), 200 μM DTT (to prevent the external cysteines from forming disulfide bonds) and 10 μM EDTA. Three to six days after injection, oocytes were stained for 2 minutes on ice with 20 μM MTS-TAMRA (Santa Cruz Biotechnology, Inc.), a fast-reacting and highly selective label that allows the attachment of a fluorescent dye to the thiol group of the introduced cysteine residue in a depolarizing K^{+} solution (in mM: 120 K-Methanesulfonate (MES), 2 $Ca(MES)_2$, and 10 HEPES, pH=7). MTS-TAMRA stock (100 mM) was dissolved in DMSO and stored at -20^{o}C. The oocytes were then thoroughly rinsed in a dye-free solution and, in some experiments, loaded with the Ca chelator BAPTA (100 nl at 10 mM, pH=7) prior to being mounted in the recording chamber.

Voltage clamp fluorometry

In developing my thesis, I have made considerable use of the voltage-clamp fluorometry technique, a powerful tool to track protein conformational rearrangements optically (Mannuzzu et al., 1996; Cha & Bezanilla, 1997). This technique takes advantage of the fact that many fluorophores are sensitive to their local environment (Lakowicz, 2006). It is possible to conjugate such fluorophores to a specific protein site and, if this area undergoes a motion that results in a change of the fluorophore environment, a deflection in the fluorescence emission will be observed. Voltage clamp fluorometry was pioneered in Shaker K^+ channels expressed in oocytes clamped by two-electrode voltage clamp (Mannuzzu et al., 1996), and was shortly after implemented in the Cut-open Oocyte Vaseline Gap (COVG) voltage clamp technique (Cha & Bezanilla, 1997).

The COVG technique (Stefani and Bezanilla, 1998; Pantazis & Olcese, 2013) is a low-noise, fast clamp technique that can allow control of the internal solution. The oocyte is mounted in a triple-compartment Perspex chamber, with a diameter of 600 μm for the top and bottom holes (Figure 7). The voltage clamp circuit is then assembled around the mounted oocyte by the placement of six salt bridges and one intracellular electrode, imposing three simultaneous voltage clamps. The three chambers are electrically-isolated by vaseline gaps: the upper chamber isolates the oocyte upper domus and maintains it under clamp; the middle chamber provides a guard shield by clamping the middle part of the oocyte to the same potential as the upper chamber; the bottom chamber allows to clamp to ground the intracellular compartment of the oocyte, through the saponin-permeabilized membrane. Changes in fluorescence signal and ionic currents were simultaneously measured from the same area of membrane isolated by the top chamber (Gandhi & Olcese, 2008). The optical setup consists of a Zeiss Axioscope FS microscope with filters

appropriate for MTS-TAMRA (Semrock). The light source is a 100 W halogen lamp. A TTL-triggered Uniblitz VS 25 shutter (Vincent Associates, Rochester, NY) is mounted on the excitation light path. The objective (Olympus LUMPlanFl, 40×, water immersion) has a numerical aperture of 0.8 and a working distance of 3.3 mm (Olympus Optical). The emission light is focused on a PIN-08-GL photodiode (UDT Technologies, Torrance, CA). A Dagan Photomax 200 amplifier is used for amplification of the photocurrent and background fluorescence subtraction.

The external solution contained (mM): 120 Na-MES (2-(N-Morpholino) ethanesulfonic acid), 10 K-MES, 2 Ca-$(MES)_2$, 10 Na-HEPES (4-(2-hydroxyethyl)-1-piperazineethanesulfonic acid) (pH=7.0). The internal solution contained (mM): 120 K-Glutamate, 10 HEPES (pH=7.0). Solution for the intracellular micro-pipette was (mM): 3000 Na-MES, 10 NaCl, and 10 HEPES (pH 7.0). Low-access resistance to the oocyte interior was obtained by permeabilizing the oocyte with 0.1% saponin dissolved in the internal solution. Experiments were conducted at temperatures of 22-24°C.

Analysis: Experimental data were analyzed with a customized program developed in the UCLA Dept. of Anesthesiology, Division of Molecular Medicine, with fitting routines running in Microsoft Excel. The G(V) curves were calculated by dividing the current-voltage relationships (I(V) curves) by the driving force (V_m-E_K), where V_m is the membrane potential and E_K the equilibrium potential for K^+, estimated from the Nernst equation. Data for the membrane conductance (G(V)) and the fluorescence (F(V)) curves were fitted to Boltzmann distributions of the form:

$$G(V) = \frac{G_{max}}{\left(1 + exp^{\frac{zF(V_{1/2} - V_m)}{RT}}\right)} - \Delta F_{min}$$

and

$$\Delta(F(V)) = \frac{\Delta F_{max} - \Delta F_{min}}{\left(1 + exp^{\frac{zF(V_{1/2} - V_m)}{RT}}\right)} - \Delta F_{min}$$

where G_{max} and F_{max} are the maximal G and F; F_{min} is the minimal F; z is the effective valence of the distribution; V_{half} is the half-activating potential; V_m is the membrane potential; F, R and T are the usual thermodynamic values. For each experiment, G(V) and F(V) curves were constructed.

Patch clamp

The patch clamp technique makes possible the measurement of ionic currents passing through ion channels (Neher & Sakmann, 1976; Sakmann & Neher, 1984; Neher & Sakmann, 1992). In this technique a small heat-polished glass pipette is pressed against the cell membrane where the ion channels are embedded and forms an electrical seal with a resistance of ~1-10 GΩ (Hamill et al., 1981). The high resistance of the seal ensures that most of the current originating in a small patch of membrane flows through the pipette, and from there to current-measurement circuitry. An electrode (a silver wire coated with AgCl), located inside the glass pipette and connected to the circuitry, converts the ionic current into electrical current. This configuration is defined as cell-attached. Other possible configurations are (Horn and Patlak, 1980; Hamill et al., 1981; Neher and Sakmann, 1992):

(1) inside-out configuration, where the pipette is rapidly withdrawn from the cell-attached configuration without destroying the giga-Ωseal, leaving a cell-free membrane and allowing current recordings in known intracellular solutions;

(2) whole-cell configuration, where after giga-seal formation the membrane patch is disrupted providing a direct low resistance access to the cell interior allowing for recordings from the ion channels in the whole cell membrane;

(3) outside-out configuration, where the pipette is gently withdrawn from the whole-cell configuration without destroying the giga-Ω seal, leaving a cell-free membrane patch exposing the outer leaflet of the lipid bilayer to the bathing solution;

(4) perforated patch, where the pipette contains specific antibiotics (such as gramicidin, anphotericin B or nystatin) that, once inserted in the plasma membrane, provide electrical access to the cell interior while preserving the cytoplasm content.

Detailed protocol for patch clamp experiments reported in this thesis:

BK channels were overexpressed in *Xenopus* oocytes. One to two days after injection, the vitelline layer of the oocytes was removed with two forceps to expose the plasma membrane. Membrane patches in the inside-out configuration were perfused with bath solutions containing (mM) 115 K-MES, 5 KCl, 5 HEDTA (N-(hydroxyethyl)-ethylenediaminetriacetic acid), 10 HEPES (pH 7.0). The [Ca^{2+}] in this solution was varied by adding $CaCl_2$. The free [Ca^{2+}] was first theoretically calculated with WEBMAXC v2.10 (http://www.stanford.edu/~cpatton/maxc.html) and then measured with a Ca^{2+} electrode (WPI, Sarasota, FL). The borosilicate glass pipettes (WPI, Sarasota, FL) were filled with the bath solution at the lowest free [Ca^{2+}] (~0.09 μM). The input resistance of electrodes was between 1.5 and 2.5 MΩ. After measuring the I-V curve with a voltage ramp from -180 mV to 100mV, the seal was excised by giving a short exposure to negative pressure. Experiments shown in this thesis were done in the inside-out configuration. The holding potential was 0 mV. Ionic currents

were digitized at 5 kHz and filtered at 1 kHz. G(V) curves were obtained for different BK clones (hSlo and hSlo-M691A).

Heme preparation:

Hemin, iron protoporphyrin IX chloride (Sigma-Aldrich) was used to apply heme in the experiments. Heme was dissolved in 30mM NaOH, and 1mM aliquots were stored at -80°C. On the day of experiment, a fresh heme tube was thawed right before use and diluted in the bath solution to the desired concentration of ~5 μM. The absorbance of the diluted heme was measured with the spectrophotometer (wavelength=385 nm, extinction coefficient=58.5 $mM^{-1}cm^{-1}$). The volume of diluted heme to add to the chamber containing 500ul of the bath solution was calculated to deliver a final concentration of 100nM. The time course of heme action was recorded by pulsing every 6 seconds at 140mV for 50ms (0mV holding potential). When the seal was stabilized, heme was applied and mixed gently. The recording was continued until the amplitude of the evoked current was in the plateau phase after the application of heme. To prevent delivering degraded heme, the diluted heme in the bath solution was used only up to 4 hours. Otherwise, fresh heme stock was prepared with the protocol described above.

CHAPTER 3: Remodeling of the BK VSD by beta1 subunits

RESULTS

The co-expression of beta1 subunit remodels the BK channel voltage sensor

The voltage clamp fluorometry technique was used to track the movement of the BK channel voltage sensors optically, in order to resolve their conformational changes during channel gating. The voltage-dependent relative arrangement of VSD segments could be established by introducing pairs of fluorophore-quenchers, which upon depolarization may move closer or away from each other (Pantazis *et al*., 2010b; Pantazis & Olcese, 2012). Thus, taking advantage of tryptophan-induced quenching, short-range protein interactions (e.g. between two VSD segments) can be measured (Mansoor et al., 2002). Fluoroscence quenching occurs when the tryptophan side chain moves toward a fluorophore by photo-induced e^- transfer upon van der Waals collision shown in Figure 8A (Mansoor et al., 2002; Pantazis and Olcese 2012). On the other hand, when Trp and a fluorophore are close to each other, this e^- transfer occurs prior to channel activation and there will be unquenching if the distance between Trp and a fluorophore increases (Pantazis and Olcese 2012).

Previous experiments indicate that the extracellular end of beta1 TM1 is in the close proximity to S1 and S2, and TM2 is in contact with S0 (Liu *et al*., 2008). In order to study the interaction between S1 on the pore forming alpha subunit and the modulatory beta1 subunit (Fig 1E), I co-expressed an alpha subunit carrying a single cysteine (for conjugation with MTS-TAMRA) at position 135 on the extracellular flank of the S1 segment. To control the calcium concentration of the oocytes, a calcium-selective chelator (BAPTA) was injected which reduced the free calcium in the cells virtually to zero. This was done because beta1 subunits show different

modulation depending on the calcium concentration (Fig 6; Orio *et al.*, 2006). Figures 8B-C show that the fluorophore labeling position S135C of the alpha subunit expressed without beta1 subunit reports voltage-dependent conformational rearrangements. The fluorescence recordings (Fig 8C) show that upon depolarization, the fluorescence increases in intensity, suggesting S4 moves away from S1 (Pantazis & Olcese, 2012). It was found that the coexpression of wild-type beta1 subunit resulted in low expression (~30uA at 120mV) but a stronger voltage-dependent unquenching of the fluorophore (Fig 8D and E), compared with the one observed for alpha subunit expressed alone. Since the fluroescence signal is generated by molecular movements, this experiment provides the first evidence that the structural rearrangements of BK channel voltage sensor are altered by the coexpression of beta1 subunit.

Beta1 perturbs BK S4 activation and pore opening

Very likely, the S1 transmembrane helix has no contribution to the voltage-sensing process of BK channels since this part of the protein has no charged amino acids (Ma et al., 2006). Pantazis and Olcese (2012) showed that the native Trp of S4 (W203) was necessary to observe changes in the voltage-dependent fluorescence from S1. Thus, I could study how beta1 association can rearrange S1 and S4 with respect to each other. In the presence of beta1 and virtually zero calcium in the cells, the voltage dependence of fluorescence change was shifted to right compared with that of alpha alone (Fig 9A). This shift (36.6 ± 0.6 mV; n=4) indicates that beta1 association in the absence of calcium promotes stabilization of the BK VSD further in the resting conformation. Figure 9B shows the mean change in fluorescence over maximum fluorescence for alpha with beta1 (5.3%) was over three times greater than those for alpha alone (1.5%). This quantitative difference in the delta-F signal is discussed below.

DISCUSSION

Fluorophore placed on the S1 segment reports an unquenching event representing the separation of S1 from S4 when the BK channel is formed by alpha subunits alone in virtually zero calcium, whereas the same position in the presence of beta1 subunit reports an increase in the voltage-dependent fluorescence change. These results provide the first evidence that the association with beta1 subunit produces an overall structural remodeling of the voltage sensor. While the precise nature of this remodeling cannot be inferred from the present results, further investigation including different pairs of site-directed labels and quenchers should provide details of the molecular reorganization.

The VSD in the presence of beta1 subunit and zero calcium results in a more stabilized resting voltage sensor state, which activates at more depolarized potentials (See Fig. 9). It is speculated that the association with beta1 alters the molecular rearrangements that underlie the VSD activation transition, destabilizing the active conformation of the voltage sensor and thus producing an overall right shift in the voltage dependence of channel gating.

How does the VSD remodeling by beta1 result in a right shift of the VSD voltage dependence?

Two of possible interpretations of the increased ΔF signal acquired from beta1-containing channels are shown in Fig. 10. Firstly, beta1 association may change the resting positions of S1 and S4, decreasing the relative distance between them. This would increase the frequency of collisions between the S1 label and S4 Trp and thus augment the quenching process. Upon depolarization, S4 departs from S1 to assume its active state, generating brighter fluorescence.

The closer proximity of S1 and S4 in the resting state may stabilize S4, hindering its activation transition. Another possible mechanism is that the beta1 association does not modify the resting positions of S1 and S4 but promotes the voltage-dependent movement of S4 towards a different active state. This position could be farther from the S1 label, resulting in increased fluorescence (Fig 10) and less stability than for the active state of beta1-less channels, which would result in a depolarizing shift of VSD activation. These hypotheses are not mutually exclusive. To test them, site-directed fluorescence labeling will be used at different positions of S1 and similar optical methods will be used to test whether beta1 association perturbs VSD activation. Also, the new direction of S4 can be determined by optically tracking its movement from positions 17, 18, 19, and 20 at the extracellular flank of S0 as well as 145 (S2) in the presence of beta1 (Pantazis *et al*., 2010b; Pantazis & Olcese, 2012). The mechanism of beta subunit modulation will be resolved by fitting data with a model of BK channel activation (Pantazis *et al*., 2010a). Furthermore, the effect of other modulatory subunits on the BK VSD can be similarly investigated and compared. Dissecting different subunit modulations can help explain the distinctive effect of beta1.

CHAPTER 4: Cytochrome C-like domain of the BK channel and modulation by heme

RESULTS

The human BK channel contains a cytochrome C-like domain

Small ligands can modulate the BK channel by binding to its intracellular Gating Ring formed by four pairs of RCK1 and RCK2 domains (Hou *et al.*, 2009). A conserved heme regulatory motif (HRM, CXXCH) typical of cytochrome C-like proteins binds heme with 68 nM kD and is located within the RCK1-RCK2 linker (Tang et al., 2003). To investigate the functional and structural similarities, sequences of the RCK1-RCK2 linker of the human BK channel and the human cytochrome C (CytC) were aligned (Fig 11A). It was found that critical elements for the function and structure of CytC were conserved in the BK linker region, including apoptotic factor 1 (Apaf1), cardiolipin, and heme-interacting residues (Fig 11A). In addition to the HRM, the second axial ligand (Met) of the heme iron was also conserved in this linker region (Fig. 11A). The axial ligands of the human CytC play a crucial role to hold the Fe atom in place (Fig. 11B). However, the role of Met 691 in the heme-dependent regulation of the BK channel remains to be elucidated. Thus, I wanted to study whether Met 691 in the BK contributes to heme binding in the following experiments.

M691 plays a crucial role in the heme-mediated regulation of BK channels

Recent studies have shown that hemin, the oxidized form of heme [Fe(II) protoporphyrin-IX], diminishes the BK currents (Horrigan *et al.*, 2005). In order to investigate whether M691 is critical for heme binding in human BK channels, this residue was substituted by Ala and the heme modulation of the mutated channels was compared to the one of WT channels.

WT and M691A mutant channels were expressed in *Xenopus* oocytes and the heme effect on BK channel activation was assessed with the patch-clamp technique in the inside-out configuration. BK channel currents were recorded at 140 mV (0 mV holding potential) every 6 seconds in the presence of 1.69 μM [Ca^{2+}]. When the K^+ current stabilized, heme was applied to the bath solution at a final concentration of 100nM. The pulse protocol persisted until a new steady-state of the K^+ currents was observed. The data were obtained following the same protocol for both WT and the mutant.

As expected, a dramatic decrease of K^+ currents was recorded from the frog oocyte overexpressing WT BK channels by the application of 100 nM heme (Fig. 12A). The concentration of heme was chosen based on the information that the estimated free heme concentration in cells is approximately 100 nM or less (Smith *et al*., 2011; Sassa, 2004). Despite the current reduction in wild-type BK, the mutant (M691A) showed a much smaller decrease in the BK currents (Fig 12B). As seen in the representative current traces, the BK current after addition of 100 nM heme was mostly abolished in the wild-type channel, with currents decreasing from ~2.5 nA to less than 0.5 nA at 140 mV (Fig 12A). On the other hand, the amplitude of the current was only diminished approximately from 2 nA to 1.7 nA in the mutant channel (Fig 12B). Furthermore, the mean fractional inhibition of BK currents by 100 nM heme confirms this effect, going from a 61.6 ± 14.6 % (n=3) decrease in the wild-type to only 13.2 ± 2.23 % (n=3) in M691A (Fig 12C). Thus, these results show that M691 is important for heme-mediated regulation of BK channels.

The BK voltage-dependent activation shift by heme was abolished with the substitution of M691

The application of 100 nM heme strongly inhibited WT BK channels (Fig. 13A and B). As previously shown (Horrigan *et al.*, 2005), 100 nM heme induced a shift towards more depolarized potentials of the mean normalized G(V) curve (n=3) (Fig 13B). The half-activating potential ($V_{1/2}$) of the wild-type changed from 81.2 ± 3.03 to 126 ± 1.67 mV (n=3) after the addition of heme (Fig 13B). Conversely, in M691 channels, the mean normalized G(V) curve (n=3) was largely unperturbed by heme addition (Fig 13D). The values of $V_{1/2}$ were nearly the same before and after heme (98.2 ± 4.13 and 100 ± 8.76 mV, Fig. 13D).

DISCUSSION

A variety of small molecules bind the BK channel (Hoshi *et al.*, 2013). Previous studies have demonstrated that intracellular heme binding modulates BK channel activity (Horrigan *et al*., 2005; Tang *et al*., 2003; Jaggar *et al*., 2005; Hou *et al*., 2009; Hou *et al*., 2006). As shown in this thesis, the functional and structural similarities of the human CytC and BK channel were investigated by aligning their sequences (Fig 11A), which indicated that in addition to the HRM, key elements of CytC were conserved in the BK channel, and that the second axial ligand to the heme iron was aligned with M691 of the BK (Fig 11A and C). These similarities suggested that the human BK channel contains four intracellular CytC-like domains.

To test if M691 in BK is critical for heme binding, the time course of 100 nM heme application on BK currents was measured from wild-type and mutant (M691A) channels. Consistent with the known effect of heme in the wild-type BK channel (Horrigan *et al.*, 2005), the reduction of BK

currents was more than 60% of the original in the presence of 100 nM heme (Fig. 12A and C). However, the observed effect of heme on the mutant was notably different from that of the wild-type (Fig 12). Using the same protocol, it was shown that the mutant exhibited a much smaller decrease in the BK currents after application of heme (Fig 12B and C). Although heme could still bind to the BK channel and diminish the K^+ currents, heme had a relatively small effect on the BK channel in the absence of M691. This result suggests that the BK channel may have markedly less affinity to heme in the absence of M691.

The normalized G(V) curves of the wild-type BK showed that the presence of 100 nM heme shifted the curve towards more depolarized membrane potentials (Fig 13B). The shift was measured to be about 45 mV, which is in good agreement with the one previously showed by Horrigan *et al.* (2005). However, the substitution of M691 almost eliminated this shift of the G(V) curves (Fig 13C). In fact, the G(V) curves of the control and 100 nM heme appear to be nearly identical. Thus, the absence of M691 may reduce the sensitivity of the BK channel to heme.

Consequences of having a CytC-like domain in the BK

Electrophysiological results in the present thesis provide the first evidence that M691 in BK is significant for BK channel modulation by heme, although the mechanisms underlying the heme sensing process by M691 needs to be delineated with further studies. The structural homology between the human CytC and the BK channel suggests that the BK channel contains a CytC-like domain (Fig 10). The hemoprotein CytC is involved in electron-transfer reactions between complexes III and IV (Kang and Crane, 2005). As the axial ligand, Met 691 with the BK CytC-

like domain may accommodate the transfer of electrons. In addition, CytC has various catalytic activities including peroxidase activity (Belikova *et al.*, 2006), suggesting a potential protective role of the BK channel for cells under oxidative stress. Binding of CytC to Apaf-1is known to be a critical point in the apoptotic program (Belikova *et al.*, 2006). It is postulated that the BK CytC-like domain may be involved in the signaling cascade of apoptosis.

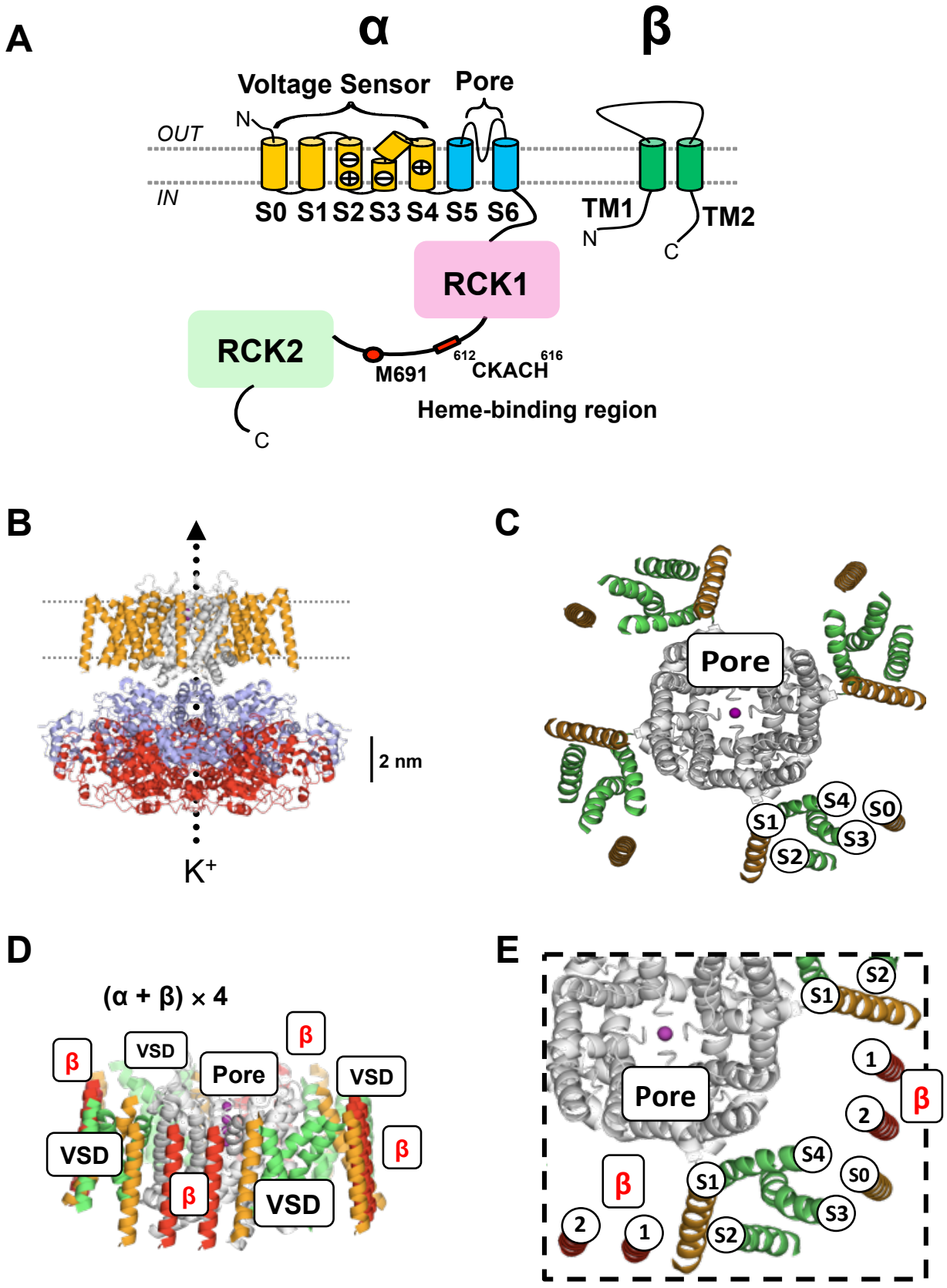
A
α
β
Voltage Sensor
Pore
OUT
IN
N
S0 S1 S2 S3 S4 S5 S6
TM1
TM2
N
C
RCK1
RCK2
M691
612
CKACH
616
Heme-binding region
C
B
2 nm
K+
C
Pore
S4
S0
S1
S3
S2
D
(α + β) × 4
β
VSD
Pore
VSD
β
VSD
β
β
VSD
E
S2
S1
1
β
2
Pore
S4
S0
β
S1
S3
2
1
S2

Figure 1. BK channel topology, putative structure and beta subunit assembly. (A) Membrane topology of BK alpha and beta subunit. In the channel-forming alpha subunit, transmembrane segments S0-S4 form a voltage sensor. Segments S5 and S6 contribute to the central, potassium-selective pore in the tetramer. The heme binding site exists between intracellular domains RCK1 and RCK2. The heme regulatory motif (HRM, CXXCH) and the putative second axial ligand (Met) to the heme Fe atom are shown in red square and circle respectively. Two transmembrane helices (TM1 and TM2) of beta subunits are connected by an extracellular loop. Note that four identical alpha subunit co-assemble in the plasma membrane to form the functional channel or associate with beta subunits with 1:1 stoichiometry. **(B)** Side view of a putative BK structure model, composed of the BK Gating Ring structure (PDB# 3NAF, red and blue), associated with the homology model of the transmemrane based on the K_V1.2-2.1 channel (PDB #2R9R), and the ideal positions of S0 helices were chosen according to Liu and coworkers (Liu *et al*., 2010; Long *et al*., 2007; Wu *et al.*, 2010). The pore domain is shown in gray, while VSD helices are shown in orange. **(C)** Top view of the BK model, formed by alpha subunits only. The pore domain is shown with K^+, ●, in the middle and surrounded by four VSDs. The charged VSD helices (S2, S3, S4, green) rearrange upon membrane depolarization (Savalli *et al*., 2006; Pantazis *et al*., 2010a; Pantazis *et al*., 2010b; Pantazis & Olcese, 2012). **(D)** BK alpha and beta subunits associate with a 1:1 stoichiometry (Knaus *et al*., 1994; Wang *et al*., 2002). **(E)** The top view of the pore and a single VSD intimately associated with beta subunits is closed-up: the TM1 of the beta subunit localizes near the S1 and S2 segments; TM2 near S0 and S4 of the adjacent alpha subunit (Wallner *et al*., 1996; Morrow *et al*., 2006; Wu *et al*., 2009; Liu *et al*., 2010; Morera *et al*., 2012; Wu *et al*., 2013).

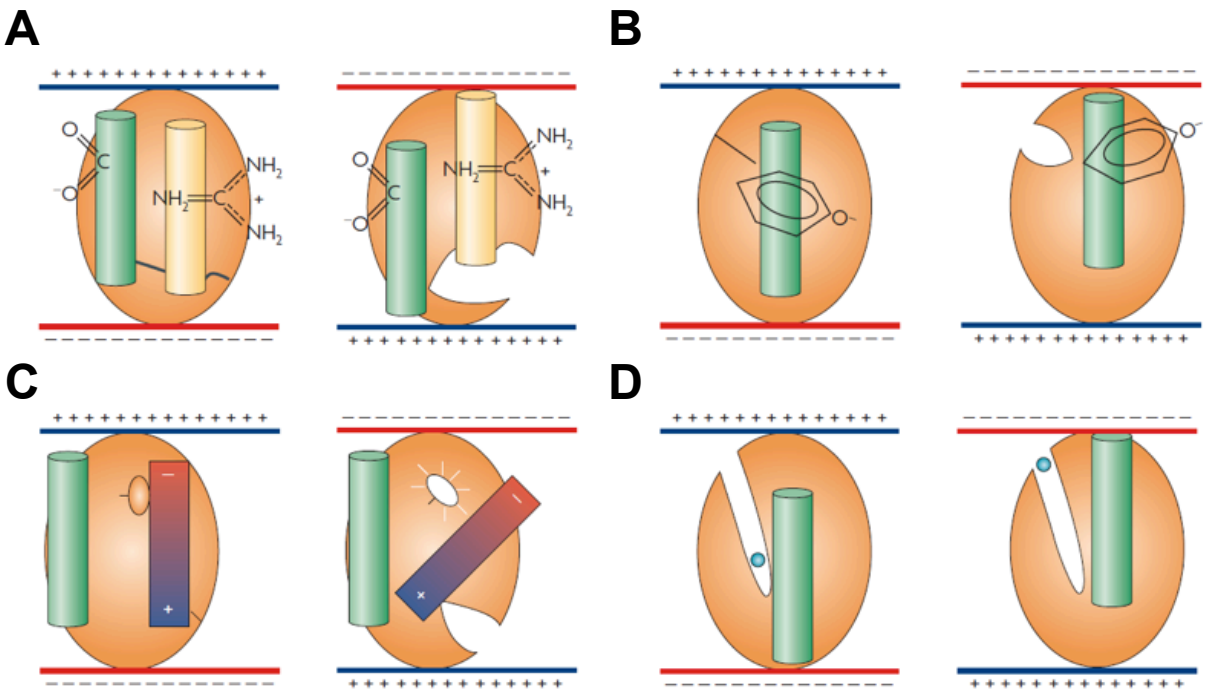

Figure 2. Possible mechanisms of voltage sensing. The simplified scheme of a transmembrane protein (orange oval) and different active sites for sensing the voltage are shown. **(A)** In response to changes in the membrane potential, charged amino acids (Asp and Arg) move within the membrane. **(B)** An intrinsic residue dipole, such as Tyr, is re-oriented through changes in the electric field. **(C)** A alpha-helix in the transmembrane contains a dipole moment (red to blue gradient) equivalent to the length of the helix that separates ± 0.5 electronic charges (e^0); the oval attached to the alpha-helix represents a fluorophore that alters emission based on the protein conformation. **(D)** Ion (light blue circle) can be re-distributed in a channel within the protein according to the electric field direction and causes a conformational change. Adapted from (Bezanilla, 2008).

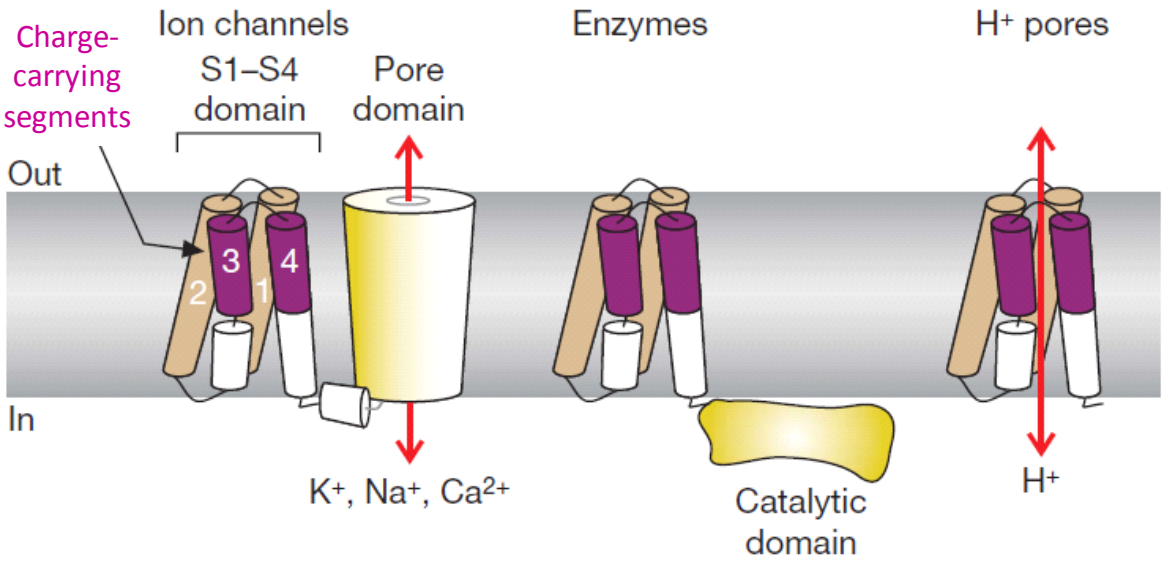

Figure 3. Scheme of S1–S4 VSDs in different membrane protein types. The S1–S4 domains (VSD) of the voltage-activated ion channels couple to an ion-selective pore domain (yellow); only one VSD out of four is shown for clarity. In enzymes such as the Ci-VSP, VSD couples to a phosphatase domain (yellow), while protons of the voltage-gated proton channels are thought to directly permeate the VSD. Adapted from (Swartz, 2008).

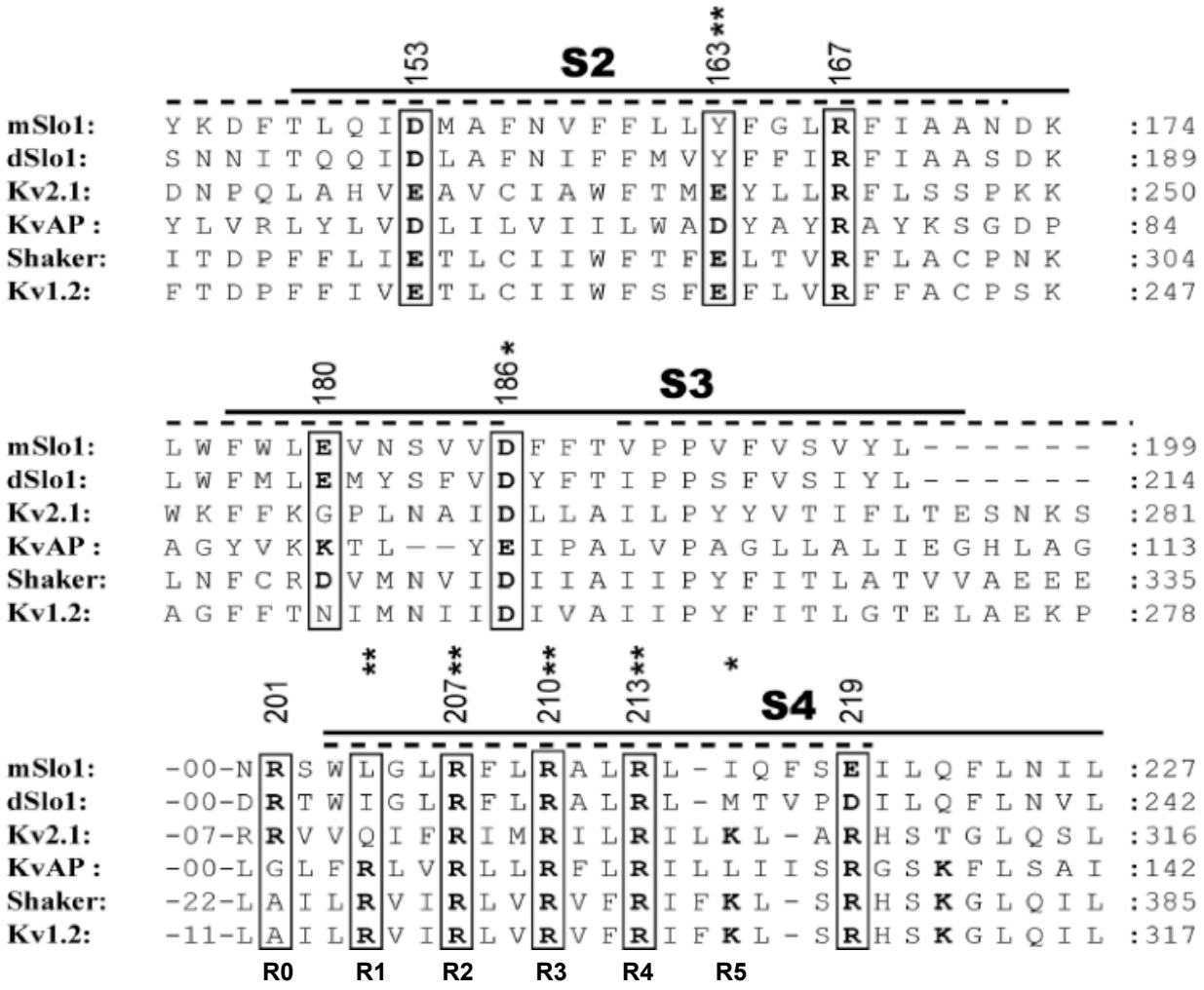

Figure 4. S2-S4 transmembrane segments of BK and K_V channels. The multiple sequence alignment of VSD from mouse and *Drosophila* BK channels (mSlo1, dSlo1, respectively) and K_V channels (K_V2.1, K_VAP, Shaker, K_V1.2) is shown (Ma et al., 2006). Transmembrane segments are marked by solid lines according to hydropathy analysis of BK (Wallner et al., 1996) and dashed lines based on the crystal structure of K_VAP (Jiang et al., 2003). Highly conserved charged residues are in bold. Star marks indicate voltage-sensing residues in Shaker. R0-R5 represent conserved positive S4 charges. Adapted from (Ma *et al*., 2006).

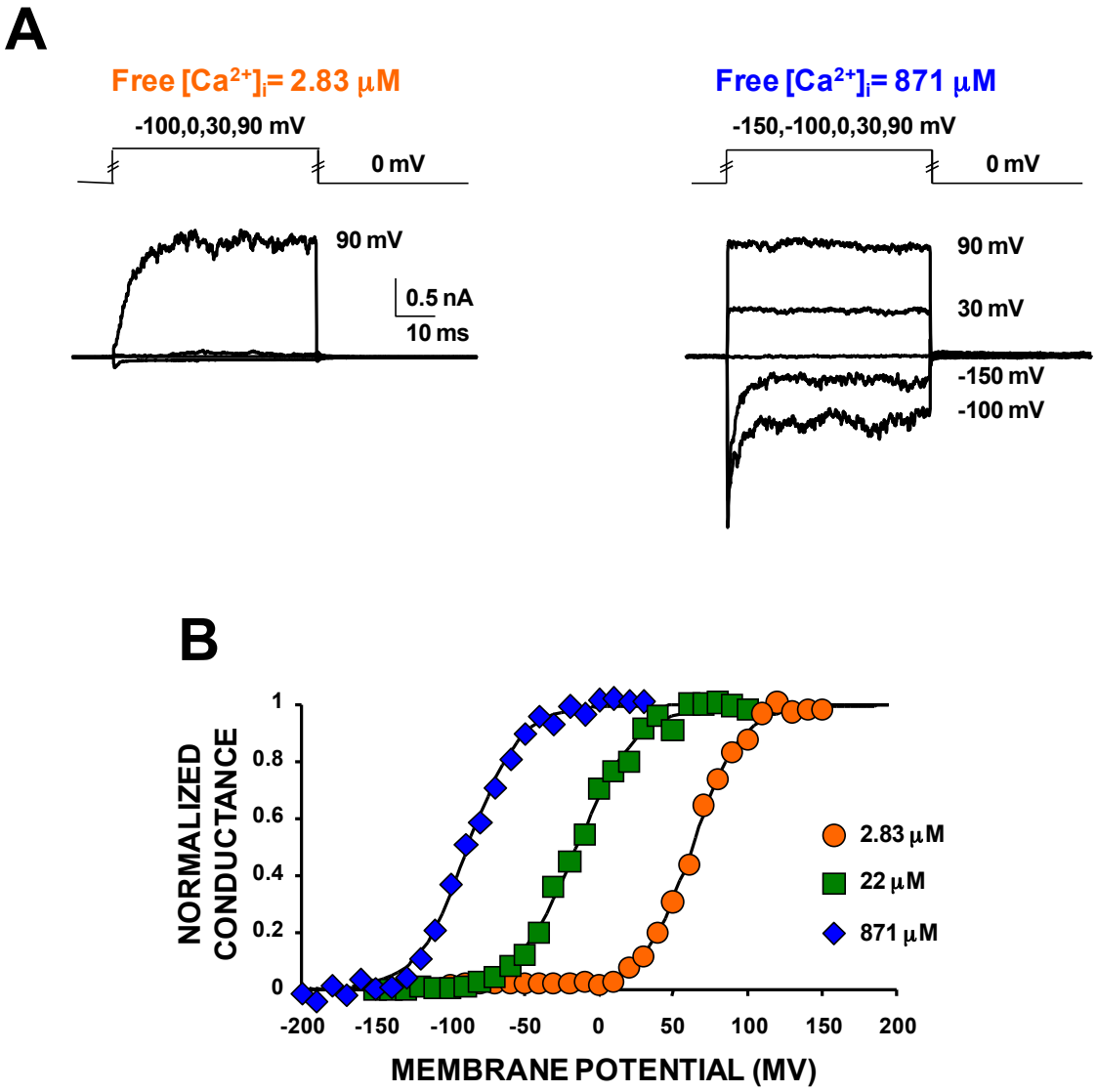

Figure 5. BK channels are activated by the voltage and/or the intracellular calcium. (A) BK current traces at various voltages are shown with two different free intracellular calcium concentrations, 2.83 μM (left) and 871 μM (right). **(B)** Normalized G(V) curves are presented in three different calcium concentrations, including 2.83 μM (orange), 22 μM (green), and 871 μM (blue). Note that G(V) curves are shifted towards more hyperpolarized potentials with greater calcium concentrations. Adapted from (Yusifov et al., 2008).

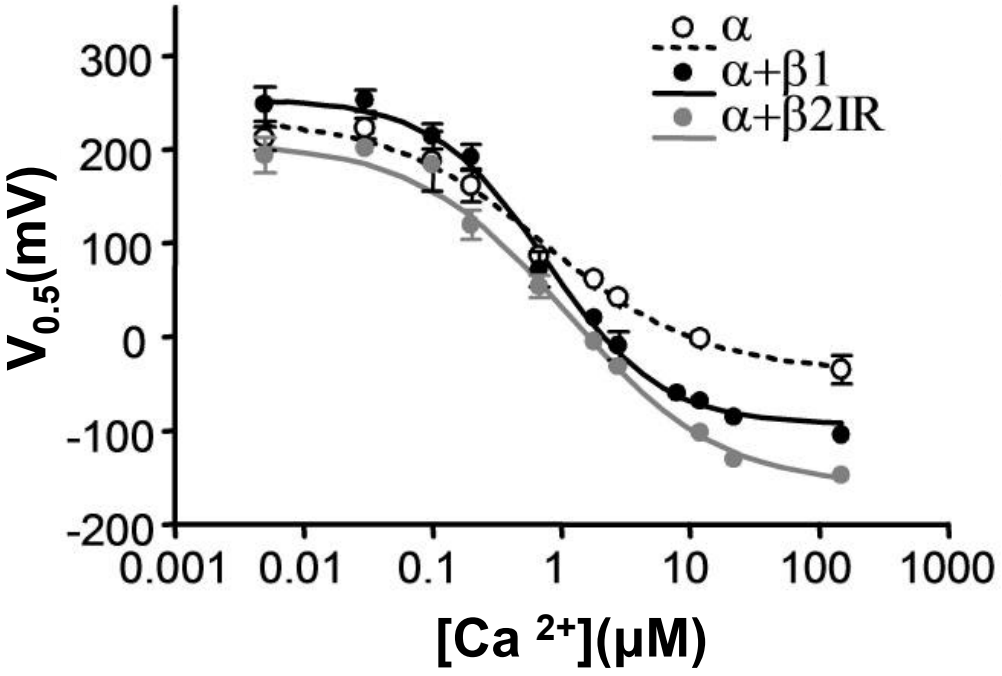

Figure 6. Beta subunits modulate the voltage-dependence of BK channels in a wide range of calcium. The obtained mean $V_{0.5}$ values are plotted against calcium concentration. The best fit sigmoid concentration–effect curves for alpha (open circles), alpha with beta 1 (closed black circles), and alpha in the presence of beta 2 IR (without the fast inactivation motif) was added as reference for visual comparison. Adapted from (Orio *et al.*, 2006).

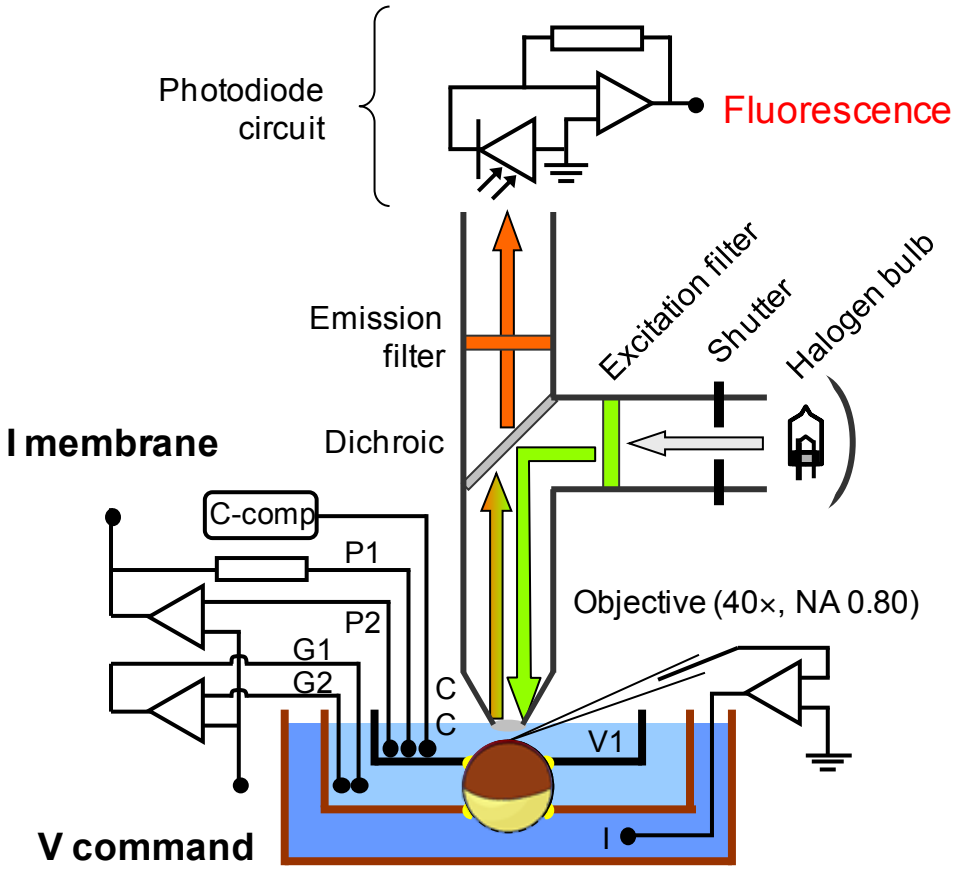

Figure 7. Cut-open Oocyte Vaseline Gap (COVG) Voltage Clamp Fluorometry. A schematic drawing of the COVG recording chambers and voltage clamp circuits, the fluorescence light path and the photodetector circuit. Fluorescence emission and ionic current are recorded simultaneously from the oocyte expressing the BK channels labeled with environment-sensitive fluorophores. Adapted from (Pantazis & Olcese, 2013).

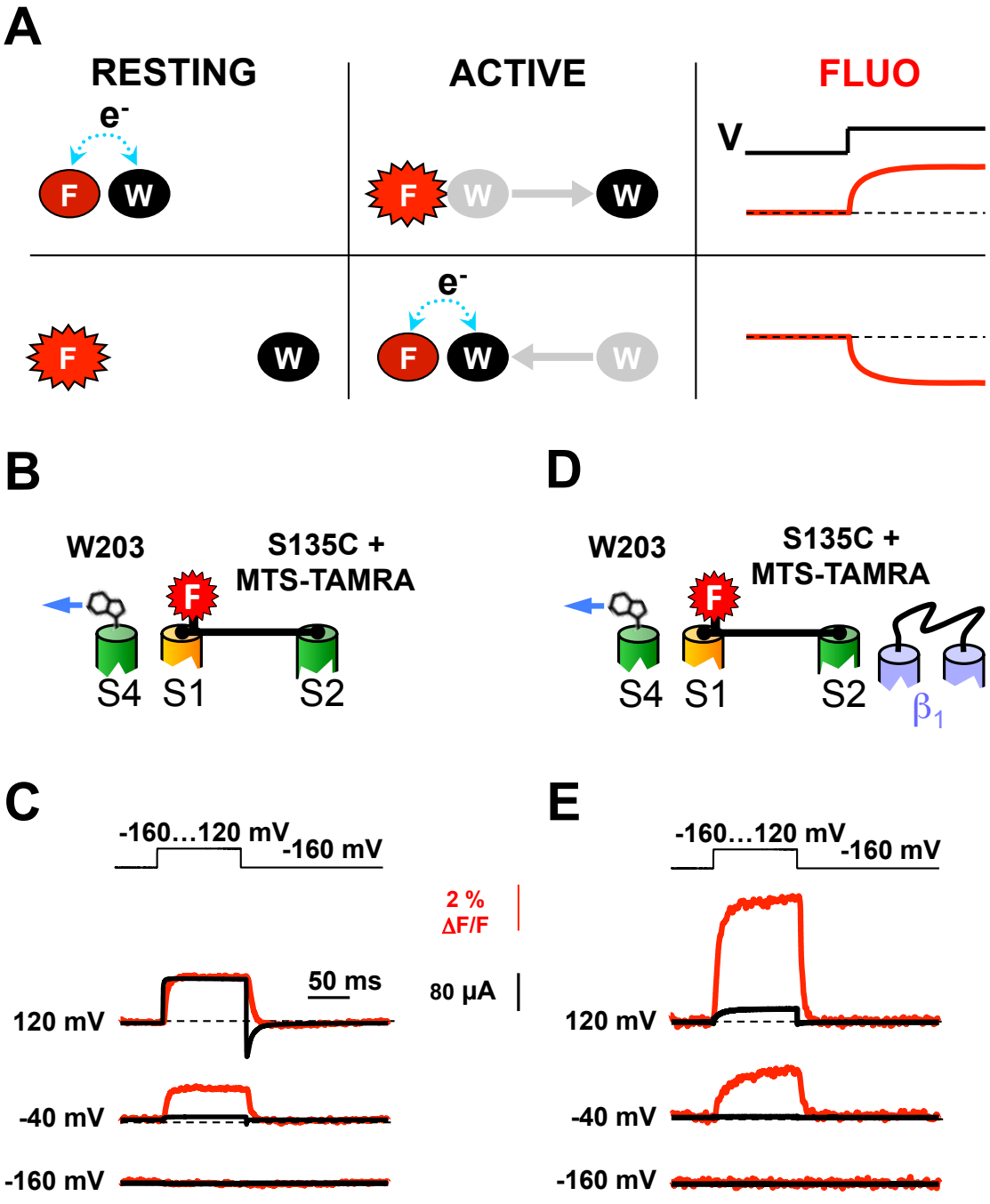
A
RESTING
ACTIVE
FLUO
e-
F
W
V
B
W203
S135C +
MTS-TAMRA
S4
S1
S2
D
β1
C
-160…120 mV
-160 mV
2 %
ΔF/F
50 ms
80 µA
120 mV
-40 mV
-160 mV
E

Figure 8. The co-expression of beta1 with BK alpha subunits perturbs the rearrangement of S4 and S1. (A) The photochemistry of Trp-mediated quenching can be used to resolve the voltage-dependent, relative movement of a Trp residue (W) and a fluorescently-labeled position (F) (Pantazis *et al*., 2010b; Pantazis and Olcese, 2012). The Trp residues collisionally quench fluorescent labels by e^- exchange (Semenova *et al*., 2009; Mansoor *et al*., 2002; Marme *et al*., 2003; Doose *et al*., 2005; Islas and Zagotta, 2006; Doose *et al*., 2009; Mansoor *et al*., 2010)=If the Trp and label diverge upon activation, the fluorescence intensity will increase because of the reduced probability of Trp/label quenching (Top). Fluorescence reduction upon membrane depolarization reports the approach of the Trp and label during activation. **(B)** BK constructs are illustrated as a simplified scheme, showing only the extracellular flanks of S1, S2 and S4 helices. A cysteine at the extracellular flank of S1 was substituted and labeled with fluorophore (MTS-TAMRA) to resolve conformational rearrangements from this region. **(C)** The representative BK current and fluorescence (red) traces recorded simultaneously are shown at the same voltage. **(D,E)** as in (B) and (C), respectively, in the presence of beta1. Note that all experiments were done in the virtual zero internal calcium.

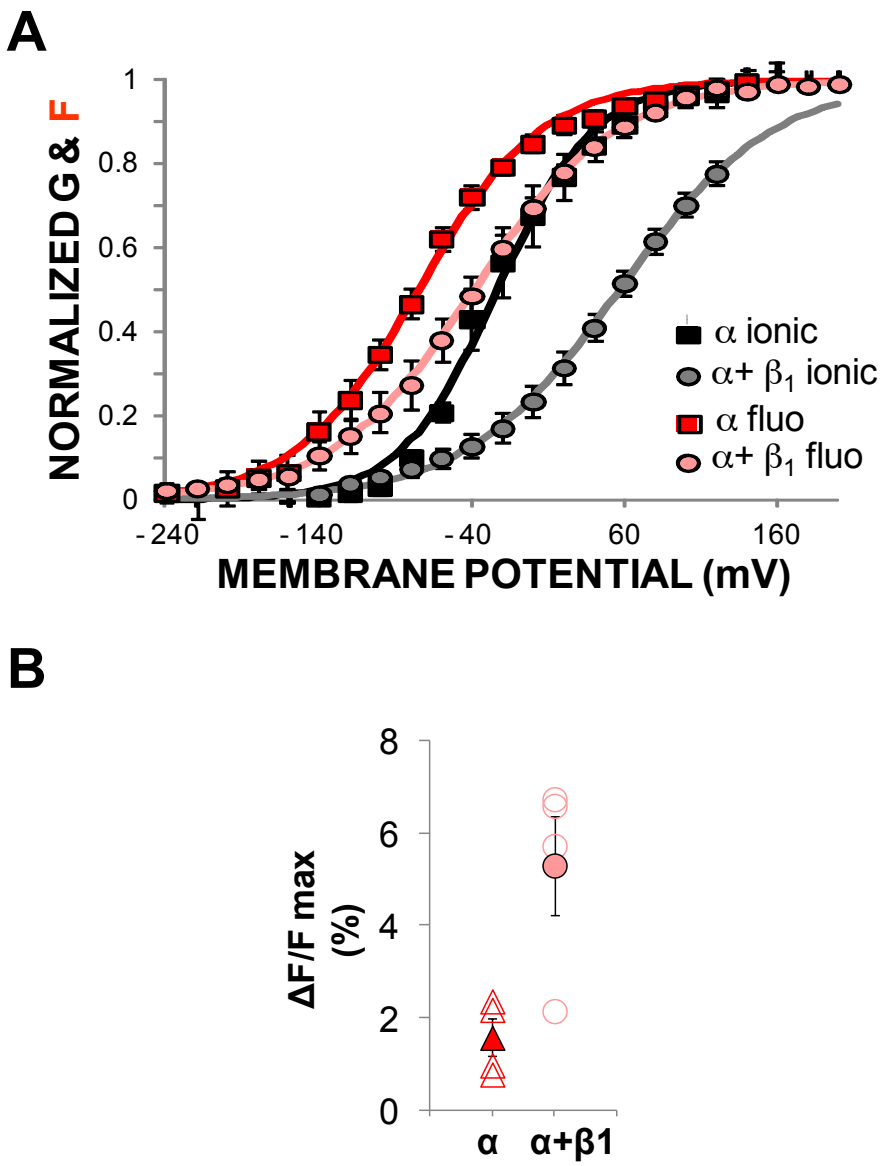

Figure 9. Beta1-induced VSD remodeling hinders BK S4 activation and pore opening. (A) Mean, normalized Conductance voltage dependence (G(V)) and changes in fluorescence voltage dependence (F(V)) curves for alpha alone (black and red squares, respectively) and with beta1 (grey and pink circles, respectively).G(V): alpha, -22.7 ± 6 mV and 0.80 ± 0.04 e^0 (n=4); alpha with beta 1, 57.3 ± 6.0 mV and 0.50 ± 0.07 e^0 (n=4). F(V): alpha, -74.3 ± 1.6 mV and 0.63 ± 0.03 e^0; alpha with beta 1, -37.8 ± 9.0 mV and 0.50 ± 0.04 e^0. **(B)** Mean fitted changes in fluorescence/ maximum fluorescence (%) from A are 1.5 ± 0.40 (n=4) and 5.3 ± 1.1 (n=4) for alpha and alpha with beta 1 respectively. Errors are S.E.M.

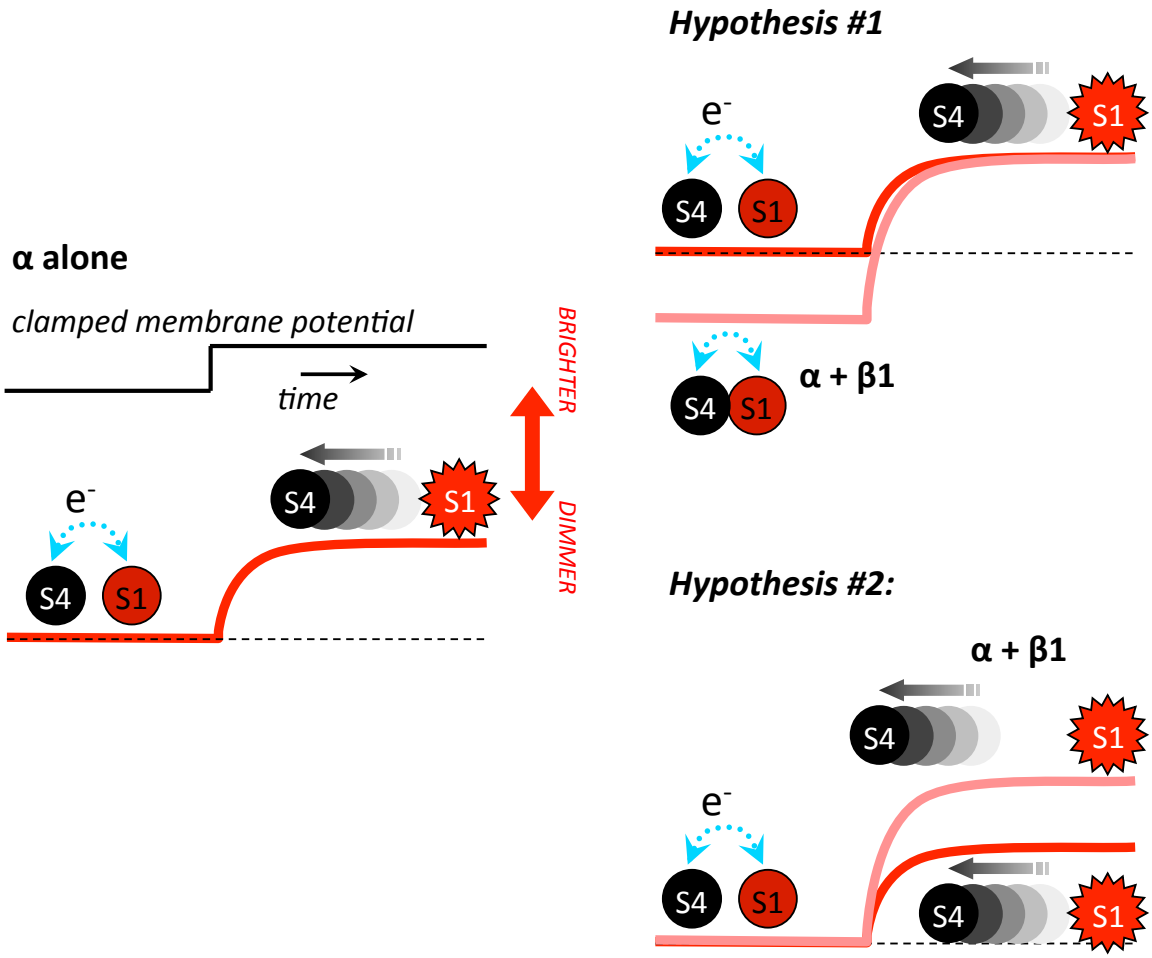

Figure 10. The relative distance between S1 and S4 increases in the presence of beta 1 subunit. Two of possible interpretations for the increase in fluorescence (Figure 9B) are shown as a scheme. Upon the depolarization of the membrane, S4 moves farther away from S1 resulting in the brighter fluorescence in the presence of beta1 (Fig.9B). The first hypothesis shows that beta 1 association decreases the distance between S1 and S4 (top) in the resting state so there is more quenching and fluorescence decrease in intensity. The delta-F is higher because the total relative divergence distance between S1 and S4 is increased. In the second hypothesis, the resting positions of S4 and S1 in beta1-containing channels do not differ from those without beta1, but S4 moves further away from S1 with depolarization, resulting in less quenching of the S1 label by the S4 Trp, hence higher delta-F.

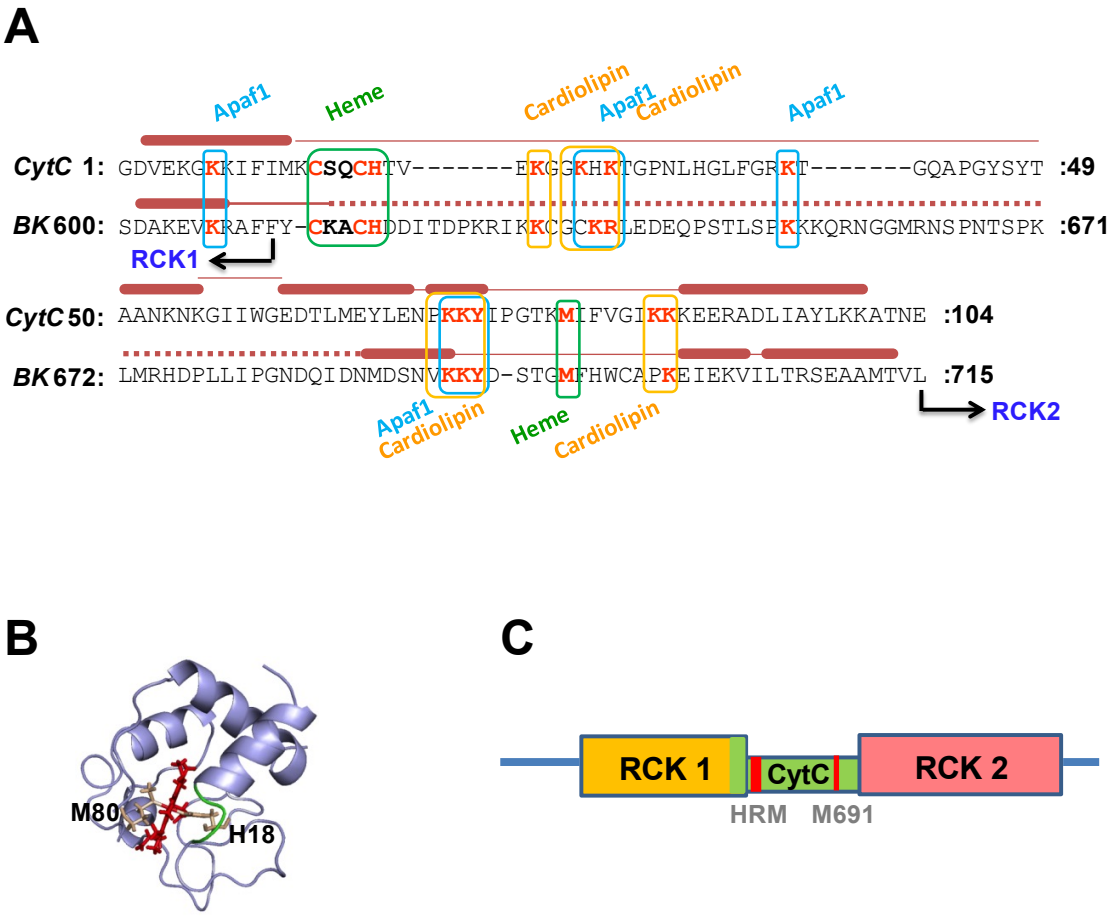

Figure 11. A putative cytochrome C (CytC)-like domain within the human BK channel. (A) The primary sequence alignment of human CytC with the RCK1-RCK2 linker of the human BK channel is shown. Structurally unresolved regions of the BK channel are shown as dotted lines. The heme regulatory motif (HRM) (CXXCH) and the second axial ligand (Met) to the heme Fe atom are shown in green boxes. Residues important for CytC / Apoptotic Factor 1 (Apaf1) complex formation are within blue boxes, while those necessary for the cardiolipin interaction of CytC are shown in orange boxes. **(B)** The human CytC in the 3D structure (PDB ID: 1J3S; Madej *et al.*, 2012). The axial ligands to the heme H18 and M80 (which may correspond to H616 and M691 in BK) are shown as sticks. **(C)** The relative position of CytC-like domain between RCK1 and RCK2 is indicated with green. The HRM and M691 are shown as red bars.

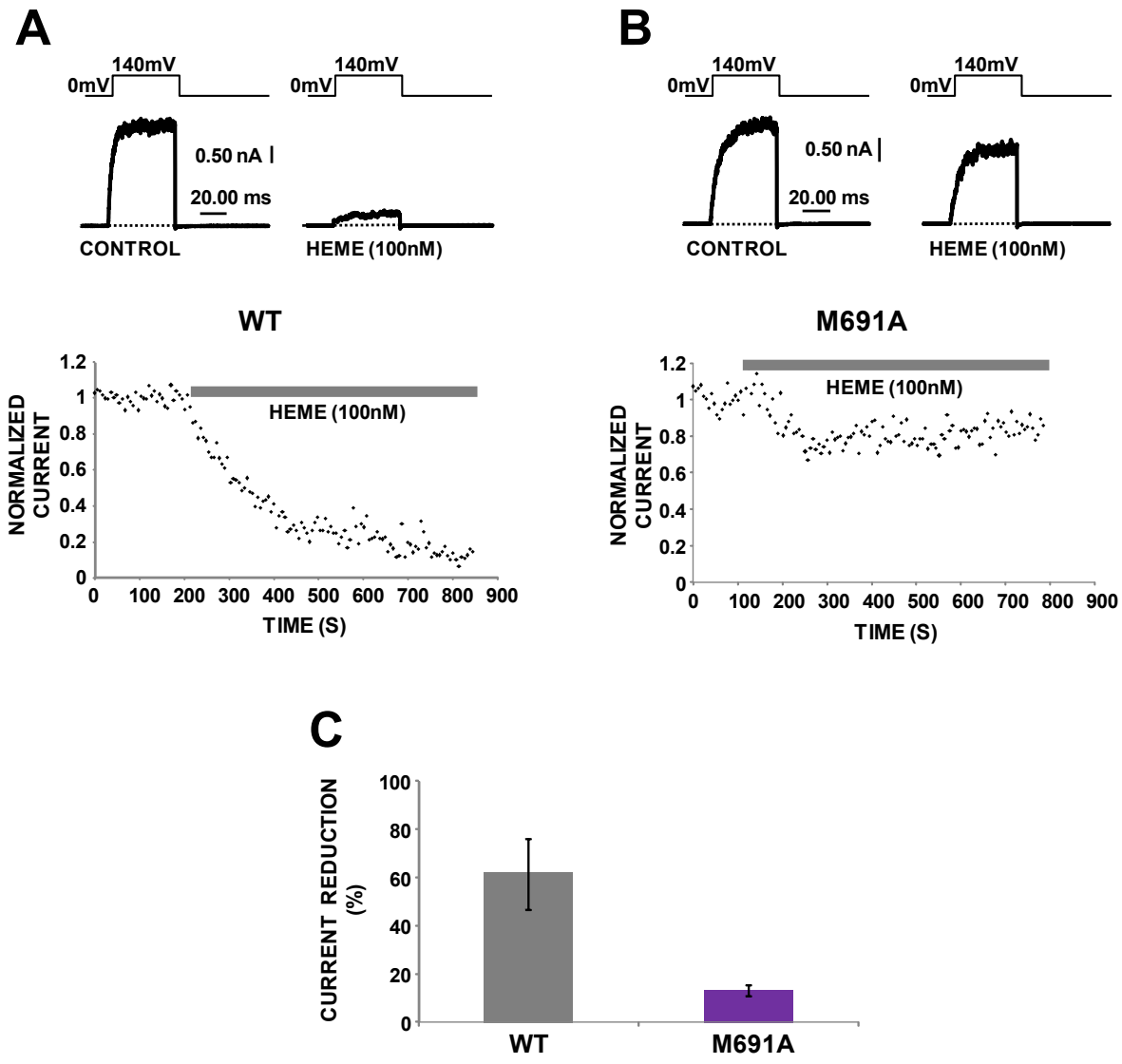

Figure 12. M691 is critical for the reduction of the BK currents by heme. (A) Representative currents from wild-type (WT) BK currents Obtained from *Xenopus* oocytes excised patches, elicited by pulses from 0 to 140 mV shown before (left) and after (right) heme (100nM) perfusion for 660 s. **(B)** WT BK inhibition by heme is plotted with the scaled peak current amplitude as a function of time. **(C,D)** As in (A) and (B), respectively, from BK channels with mutation M691A. **(C)** The mean fractional inhibition of K^+ currents from WT and M691A channels is plotted as bar graphs with error bars (SEM). The percentages of the current reductions for WT and M691A were 61.6 ± 14.6 % and 13.2 ± 2.23 % respectively (n=3).

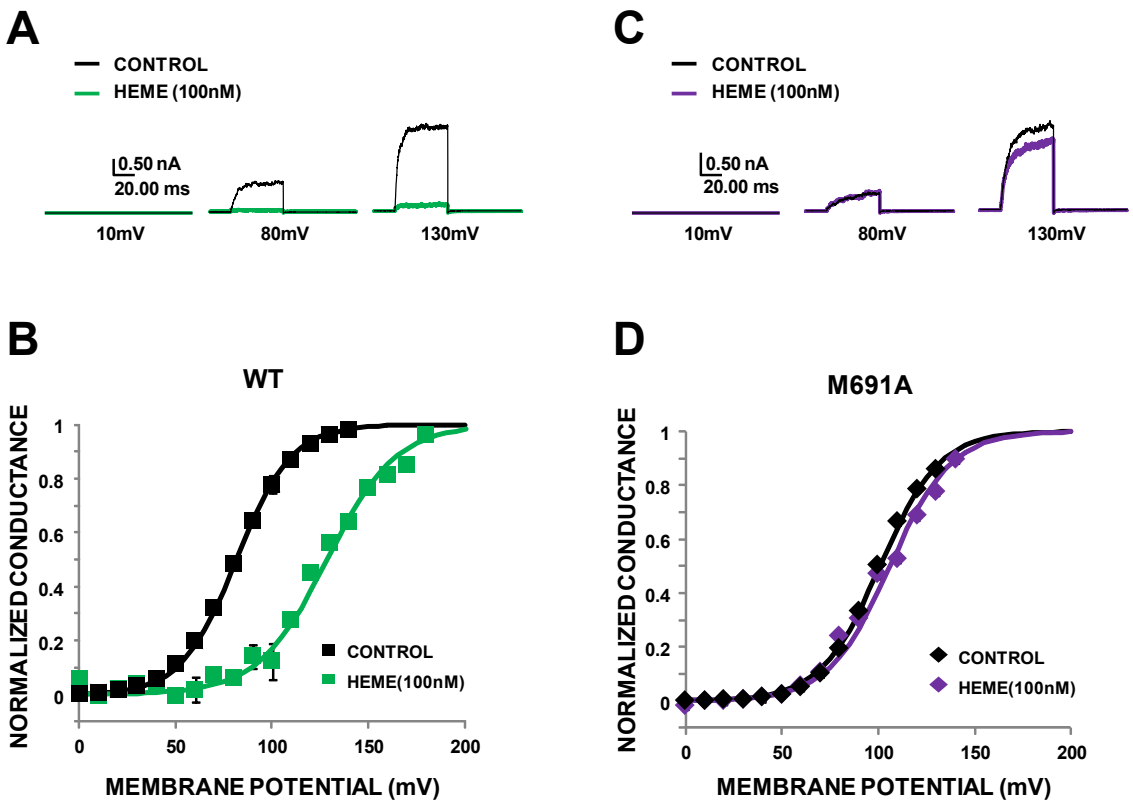

Figure 13. M691A abolishes the effect of heme on the voltage-dependence of BK macroscopic conductance. (A) Representative current traces of WT BK channels recorded at different voltages before and after application of heme (100nM; green traces). **(B)** Mean, normalized G-V curves from WT BK. **(C,D)** As in (A) and (B), respectively from the mutant BK channels (M691A). Note that representative current traces of BK channels with M691A mutation after heme are shown in purple traces in (C). Error bars (within the symbols when not visible) represent SEM. The values of $V_{0.5}$ and z for the WT control group were 81.2 ± 3.03 mV and 1.68 ± 0.12 e^0 and those for the heme group were 126 ± 1.67 mV and 1.38± 0.09 e^0 (n=3). For M691A, $V_{0.5}$ and z for the control group were 98.2 ± 4.13 mV and 1.88 ± 0.03 e^0 and those for the heme group were 100 ± 8.76 mV and 1.59 ± 0.05 e^0 (n=3).

REFERENCES

Alberts B, Johnson A, Lewis J, et al. Molecular Biology of the Cell. 4th edition. New York: Garland Science; 2002. Ion Channels and the Electrical Properties of Membranes.

Armstrong CM (2003). Voltage-gated K channels. *Sci STKE* 2003, re10.

Belikova NA, Vladimirov YA, Ospipov AN, Kapralov AA, Tyurin VA, Potapovich MV, Basova LV, Peterson J, Kurnikov IV, Kagan VE (2006). Peroxidase Activity and Structural Transitions of cytochrome c Bound to Cardiolipin-Containing Membranes. *Biochem* 45(15): 4998–5009.

Bezanilla,F (2008). How membrane proteins sense voltage. *Nat Rev Mol Cell Biol* 9:323-332.

Brenner R, Perez GJ, Bonev AD, Eckman DM, Kosek JC, Wiler SW, Patterson AJ, Nelson MT, & Aldrich RW (2000). Vasoregulation by the beta1 subunit of the calcium-activated potassium channel. *Nature* 407, 870-876.

Budelli G, Geng Y, Butler A, Magleby KL, & Salkoff L (2013). Properties of Slo1 K+ channel with and without the gating ring. *Proc Natl Acad Sci U S A* 110, 16657-16662.

Cha,A. and F.Bezanilla (1997). Characterizing voltage-dependent conformational changes in the Shaker K+ channel with fluorescence. *Neuron* 19:1127-1140.

Colwell CS (2011). Linking neural activity and molecular oscillations in the SCN. *Nat Rev Neurosci* 12(10):553-69.

Contreras GF, Neely A, Alvarez O, Gonzalez C, & Latorre R (2012). Modulation of BK channel voltage gating by different auxiliary beta subunits. *Proc Natl Acad Sci U S A* 109, 18991-18996.

Cui J (2010). BK-type calcium-activated potassium channels: coupling of metal ions and voltage sensing. *J Physiol*.

Cui J, Yang H, & Lee US (2009). Molecular mechanisms of BK channel activation. *Cell Mol Life Sci* 66, 852-875.

Diaz L, Meera P, Amigo J, Stefani E, Alvarez O, Toro L, & Latorre R (1998). Role of the S4 segment in a voltage-dependent calcium-sensitive potassium (hSlo) channel. *J Biol Chem* 273, 32430-32436.

Doose S, Neuweiler H, Sauer M (2005). A close look at fluorescence quenching of organic dyes by tryptophan. *Chemphyschem* 6:2277-2285.

Doose S, Neuweiler H, Sauer M (2009). Fluorescence quenching by photoinduced electron transfer: a reporter for conformational dynamics of macromolecules. *Chemphyschem* 10:1389-1398.

Du W, Bautista JF, Yang H, ez-Sampedro A, You SA, Wang L, Kotagal P, Luders HO, Shi J, Cui J, Richerson GB, & Wang QK (2005). Calcium-sensitive potassium channelopathy in human epilepsy and paroxysmal movement disorder. *Nat Genet* 37, 733-738.

Fain GL (2011). Adaptation of mammalian photoreceptors to background light: putative role for direct modulation of phosphodiesterase. *Mol Neurobiol.* 44, 374-382.

Gandhi,C.S. & Olcese R (2008). The Voltage-Clamp Fluorometry Technique. *In* Methods in Molecular Biology, Potassium Channels. J.D.Lippiat, editor. Humana Press, Totowa. 213-231.

Grimm PR & Sansom SC (2010). BK channels and a new form of hypertension. *Kidney Int* 78, 956-962.

Hamill,O.P., Marty A, Neher E, Sakmann B, & Sigworth FJ (1981). Improved patch-clamp techniques for high-resolution current recording from cells and cell-free membrane patches. *Pflugers Arch.* 391:85-100.

Hille B (2001). Ion channels of excitable membranes. Sinauer associates, 3rd edition

Horn,R. & J.Patlak (1980). Single channel currents from excised patches of muscle membrane. *Proc. Natl. Acad. Sci. U. S. A* 77:6930-6934.

Horrigan FT & Aldrich RW (1999). Allosteric voltage gating of potassium channels II. Mslo channel gating charge movement in the absence of Ca(2+). *J Gen Physiol* 114, 305-336.

Horrigan FT & Aldrich RW (2002). Coupling between voltage sensor activation, Ca2+ binding and channel opening in large conductance (BK) potassium channels. *J Gen Physiol* 120, 267-305.

Horrigan FT, Cui J, & Aldrich RW (1999). Allosteric voltage gating of potassium channels I. Mslo ionic currents in the absence of Ca(2+). *J Gen Physiol* 114, 277-304.

Horrigan FT, Heinemann SH, & Hoshi T (2005). Heme regulates allosteric activation of the Slo1 BK channel. *J Gen Physiol* 126, 7-21.

Horrigan FT & Hoshi T (2008). Integration of an electric-metal sensory experience in the Slo1 BK channel. *Nat Struct Mol Biol* 15, 1130-1132.

Hoshi T, Pantazis A, & Olcese R (2013). Transduction of voltage and Ca2+ signals by Slo1 BK channels. *Physiology (Bethesda)* 28, 172-189.

Hou S, Heinemann SH, & Hoshi T (2009). Modulation of BKCa channel gating by endogenous signaling molecules. *Physiology (Bethesda)* 24, 26-35.

Hou S, Reynolds MF, Horrigan FT, Heinemann SH, Hoshi T (2006). Reversible binding of heme to proteins in cellular signal transduction. *Acc Chem Res* 39(12):918-924.

Hu L, Shi J, Ma Z, Krishnamoorthy G, Sieling F, Zhang G, Horrigan FT, & Cui J (2003). Participation of the S4 voltage sensor in the Mg2+-dependent activation of large conductance (BK) K+ channels. *Proc Natl Acad Sci U S A* 100, 10488-10493.

Islas LD & Zagotta WN (2006). Short-range molecular rearrangements in ion channels detected by tryptophan quenching of bimane fluorescence. *J Gen Physiol* 128:337-346.

Jaggar JH, Li A, Parfenova H, Liu J, Umstot ES, Dopico AM, & Leffler CW (2005). Heme is a carbon monoxide receptor for large-conductance Ca2+-activated K+ channels. *Circ Res* 97, 805-812.

Javaherian AD, Yusifov T, Pantazis A, Franklin S, Gandhi CS, & Olcese R (2011). Metal-driven operation of the human large-conductance voltage- and Ca2+- dependent potassium channel (BK) gating ring apparatus. *J Biol Chem* 286, 20701-20709.

Jensen MO, Jogini V, Borhani DW, Leffler AE, Dror RO, & Shaw DE (2012). Mechanism of voltage gating in potassium channels. *Science* 336, 229-233.

Jiang,Y, Lee A, Chen J, Ruta V, Cadene M, Chait BT, & MacKinnon R (2003). X-ray structure of a voltage-dependent K+ channel. *Nature* 423:33-41.

Jiang Z, Wallner M, Meera P, & Toro L (1999). Human and rodent MaxiK channel beta-subunit genes: cloning and characterization. *Genomics* 55, 57-67.

Kang SA & Crane BR (2005). Effects of interface mutations on association modes and electron-transfer rates between proteins. *Proc Natl Acad Sci* U S A. 102:15465–70.

Knaus HG, Garcia-Calvo M, Kaczorowski GJ, & Garcia ML (1994). Subunit composition of the high conductance calcium-activated potassium channel from smooth muscle, a representative of the mSlo and slowpoke family of potassium channels. *J Biol Chem* 269:3921-3924.

Kuhlman S, & McMahon D (2004). Rhythmic regulation of membrane potential and potassium current persists in SCN neurons in the absence of encironmental input. *Eur. J Neurosci* 20, 1113-1117.

Kuhlman S, & McMahon D (2006). Encoding the ins and outs of circadian pacemaking. *J Biol Rhythms* 21, 470-481.

Lakowicz,J.R. (2006). Principles of Fluorescence Spectroscopy. 3rd ed. Springer, New York, NY. -954 pp.

Latorre R & Brauchi S (2006). Large conductance Ca2+-activated K+ (BK) channel: activation by Ca2+ and voltage. *Biol Res* 39, 385-401.

Latorre R, Morera FJ, & Zaelzer C (2010). Allosteric interactions and the modular nature of the voltage- and Ca2+-activated (BK) channel. *J Physiol* 588, 3141-3148.

Ledoux J, Werner ME, Brayden JE, & Nelson MT (2006). Calcium-activated potassium channels and the regulation of vascular tone. *Physiology (Bethesda)* 21, 69-78.

Lee US & Cui J (2010). BK channel activation: structural and functional insights. *Trends Neurosci* 33, 415-423.

Lee US, Shi J, & Cui J (2010). Modulation of BK channel gating by the ss2 subunit involves both membrane-spanning and cytoplasmic domains of Slo1. *J Neurosci* 30, 16170-16179.

Lehmann-Horn F & Jurkat-Rott K (1999). Voltage-gated ion channels and hereditary disease. *Physiol Rev* 79, 1317-1372.

Leonetti MD, Yuan P, Hsiung Y, & Mackinnon R (2012). Functional and structural analysis of the human SLO3 pH- and voltage-gated K+ channel. *Proc Natl Acad Sci U S A* 109, 19274-19279.

Liu,G., X.Niu, R.S.Wu, N.Chudasama, Y.Yao, X.Jin, R.Weinberg, S.I.Zakharov, H.Motoike, S.O.Marx, & A.Karlin (2010). Location of modulatory {beta} subunits in BK potassium channels. *J. Gen. Physiol*.

Liu G, Zakharov SI, Yang L, Wu RS, Deng SX, Landry DW, Karlin A, & Marx SO (2008). Locations of the β1 transmembrane helices in the BK potassium channel. *Proc. Natl. Acad. Sci. U. S. A* 105:10727-10732.

Long,S.B., X.Tao, E.B.Campbell, & R.MacKinnon. (2007). Atomic structure of a voltage-dependent K+ channel in a lipid membrane-like environment. *Nature* 450:376-382.

Ma Z, Lou XJ, & Horrigan FT (2006). Role of charged residues in the S1-S4 voltage sensor of BK channels. *J Gen Physiol* 127, 309-328.

Madej T, Addess KJ, Fong JH, Geer LY, Geer RC, Lanczycki CJ, Liu C, Lu S, Marchler-Bauer A, Panchenko AR, Chen J, Thiessen PA, Wang Y, Zhang D, Bryant SH. "MMDB: 3D structures and macromolecular interactions." Nucleic Acids Res. 2012 Jan; 40(Database issue):D461-4

Mannuzzu,L.M., M.M.Moronne, & E.Y.Isacoff (1996). Direct physical measure of conformational rearrangement underlying potassium channel gating. *Science* 271:213-216.

Mansoor SE, McHaourab HS, Farrens DL (2002). Mapping proximity within proteins using fluorescence spectroscopy. A study of T4 lysozyme showing that tryptophan residues quench bimane fluorescence. *Biochemistry* 41:2475-2484.

Mansoor SE, Dewitt MA, Farrens DL (2010). Distance mapping in proteins using fluorescence spectroscopy: the tryptophan-induced quenching (TrIQ) method. *Biochemistry* 49:9722-9731.

Marme N, Knemeyer JP, Sauer M, Wolfrum J (2003). Inter- and intramolecular fluorescence quenching of organic dyes by tryptophan. *Bioconjug Chem* 14:1133-1139.

Meredith AL, Wiler SW, Miller BH, Takahashi JS, Fodor AA, Ruby NF, & Aldrich RW (2006). BK calcium-activated potassium channels regulate circadian behavioral rhythms and pacemaker output. *Nat Neurosci* 9, 1041-1049.

Miranda P, Contreras JE, Plested AJ, Sigworth FJ, Holmgren M, & Giraldez T (2013). State-dependent FRET reports calcium- and voltage-dependent gating-ring motions in BK channels. *Proc Natl Acad Sci U S A* 110, 5217-5222.

Montgomery JR & Meredith AL (2012). Genetic activation of BK currents in vivo generates bidirectional effects on neuronal excitability. *Proc Natl Acad Sci U S A* 109, 18997-19002.

Morera FJ, Alioua A, Kundu P, Salazar M, Gonzalez C, Martinez AD, Stefani E, Toro L, & Latorre R (2012). The first transmembrane domain (TM1) of beta2-subunit binds to the transmembrane domain S1 of alpha-subunit in BK potassium channels. *FEBS Lett* 586:2287-2293.

Neher,E. & B.Sakmann. 1976. Single-channel currents recorded from membrane of denervated frog muscle fibres. *Nature* 260:799-802.

Neher,E. & B.Sakmann (1992). The patch clamp technique. *Sci. Am.* 266:44-51.

Niu,X., X.Qian, & K.L.Magleby (2004). Linker-gating ring complex as passive spring and Ca(2+)-dependent machine for a voltage- and Ca(2+)-activated potassium channel. *Neuron* 42:745-756.

Orio P & Latorre R (2005). Differential effects of beta 1 and beta 2 subunits on BK channel activity. *J Gen Physiol* 125, 395-411.

Orio P, Torres Y, Rojas P, Carvacho I, Garcia ML, Toro L, Valverde MA, & Latorre R (2006). Structural determinants for functional coupling between the beta and alpha subunits in the Ca2+-activated K+ (BK) channel. *J Gen Physiol* 127, 191-204.

Pantazis,A., V.Gudzenko, N.Savalli, D.Sigg, & R.Olcese (2010a). Operation of the voltage sensor of a human voltage- and Ca2+-activated K+ channel. *Proc. Natl. Acad. Sci. U. S A* 107:4459-4464.

Pantazis,A., A.P.Kohanteb, & R.Olcese (2010b). Relative motion of transmembrane segments S0 and S4 during voltage sensor activation in the human BK(Ca) channel. *J. Gen. Physiol* 136:645-657.

Pantazis,A. and R.Olcese (2012). Relative transmembrane segment rearrangements during BK channel activation resolved by structurally assigned fluorophore-quencher pairing. *J. Gen. Physiol* 140:207-218.

Pantazis,A. & Olcese,R. Cut-open oocyte voltage-clamp technique. In Encyclopedia of Biophysics. Roberts,G.C.K. (ed.), pp. 406-413 (Springer, Berlin, Heidelberg, 2013).

Poulsen AN, Wulf H, Hay-Schmidt A, Jansen-Olesen I, Olesen J, & Klaerke DA (2008). Differential expression of BK channel isoforms and beta-subunits in rat neurovascular tissues. *Biochimica et Biophysiica Acta (BBA)- Biomembranes*, 1788, 380-389

Ramsey,I.S., M.M.Moran, J.A.Chong, & D.E.Clapham (2006). A voltage-gated proton-selective channel lacking the pore domain. *Nature* 440:1213-1216.

Sakmann,B. & E.Neher (1984). Patch clamp techniques for studying ionic channels in excitable membranes. *Annu. Rev. Physiol* 46:455-472.

Sasaki,M., M.Takagi, & Y.Okamura (2006). A voltage sensor-domain protein is a voltage-gated proton channel. *Science* 312:589-592.

Sassa S (2004). Why heme needs to be degraded to iron, biliverdin IXα, and carbon monoxide? *Antioxid Redox Signal* 6(5):819-824.

Savalli N, Kondratiev A, de Quintana SB, Toro L, & Olcese R (2007). Modes of operation of the BKCa channel beta2 subunit. *J Gen Physiol* 130, 117-131.

Savalli,N., A.Kondratiev, L.Toro, & R.Olcese (2006). Voltage-dependent conformational changes in human Ca(2+)- and voltage-activated K(+) channel, revealed by voltage-clamp fluorometry. *Proc. Natl. Acad. Sci. U. S A* 103:12619-12624.

Savalli,N., Pantazis,A., Yusifov,T., Sigg,D. & Olcese,R (2012). The contribution of RCK domains to human BK channel allosteric activation. *J. Biol. Chem*. 287, 21741-21750.

Schreiber M & Salkoff L (1997). A novel calcium-sensing domain in the BK channel. *Biophys J* 73, 1355-1363.

Seibold MA, Wang B, Eng C, Kumar G, Beckman KB, Sen S, Choudhry S, Meade K, Lenoir M, Watson HG, Thyne S, Williams LK, Kumar R, Weiss KB, Grammer LC, Avila PC, Schleimer RP, Burchard EG, & Brenner R (2008). An african-specific functional polymorphism in KCNMB1 shows sex-specific association with asthma severity. *Hum Mol Genet* 17, 2681-2690.

Semenova NP, Abarca-Heidemann K, Loranc E, Rothberg BS (2009). Bimane fluorescence scanning suggests secondary structure near the S3-S4 linker of BK channels. *J Biol Chem* 284:10684-10693.

Shen KZ, Lagrutta A, Davies NW, Standen NB, Adelman JP, & North RA (1994). Tetraethylammonium block of Slowpoke calcium-activated potassium channels expressed in Xenopus oocytes: evidence for tetrameric channel formation. *Pflugers Arch* 426, 440-445.

Shipston MJ (2013). Regulation of large conductance calcium- and voltage-activated potassium (BK) channels by S-palmitoylation. *Biochem Soc Trans* 41, 67-71.

Smith AG, Raven EL, & Chernova T (2011). The regulatory role of heme in neurons. *Metallomics* 3(10):955-962.

Stefani,E. & F.Bezanilla (1998). Cut-open oocyte voltage-clamp technique. *Methods Enzymol.* 293:300-318.

Stefani,E., M.Ottolia, F.Noceti, R.Olcese, M.Wallner, R.Latorre, & L.Toro (1997). Voltage-controlled gating in a large conductance Ca2+-sensitive K+channel (hslo). *Proc. Natl. Acad. Sci. U. S A* 94:5427-5431.

Sun X, Zaydman MA, & Cui J (2012). Regulation of voltage-activated K+ channel gating by transmembrane beta subunits. *Front Pharmacol.* 3, 63.

Swartz,K.J. (2008). Sensing voltage across lipid membranes. *Nature* 456:891-897.

Tang XD, Garcia ML, Heinemann SH, & Hoshi T (2004). Reactive oxygen species impair Slo1 BK channel function by altering cysteine-mediated calcium sensing. *Nat Struct Mol Biol* 11, 171-178.

Tang XD, Xu R, Reynolds MF, Garcia ML, Heinemann SH, & Hoshi T (2003). Haem can bind to and inhibit mammalian calcium-dependent Slo1 BK channels. *Nature* 425, 531-535.

Uebele VN, Lagrutta A, Wade T, Figueroa DJ, Liu Y, McKenna E, Austin CP, Bennett PB, & Swanson R (2000). Cloning and functional expression of two families of beta-subunits of the large conductance calcium-activated K+ channel. *J Biol Chem* 275, 23211-23218.

Wallner M, Meera P, Ottolia M, Kaczorowski GJ, Latorre R, Garcia ML, Stefani E, & Toro L (1995). Characterization of and modulation by a beta-subunit of a human maxi KCa channel cloned from myometrium. *Receptors Channels* 3, 185-199.

Wallner M, Meera P, & Toro L (1996). Determinant for beta-subunit regulation in high-conductance voltage-activated and Ca(2+)-sensitive K+ channels: an additional transmembrane region at the N terminus. *Proc Natl Acad Sci U S A* 93, 14922-14927.

Wallner M, Meera P, & Toro L (1999). Molecular basis of fast inactivation in voltage and Ca2+-activated K+ channels: a transmembrane beta-subunit homolog. *Proc Natl Acad Sci U S A* 96, 4137-4142.

Wang YW, Ding JP, Xia XM, & Lingle CJ (2002). Consequences of the stoichiometry of Slo1 alpha and auxiliary beta subunits on functional properties of large-conductance Ca2+-activated K+ channels. *J Neurosci* 22:1550-1561.

Wei A, Solaro C, Lingle C, & Salkoff L (1994). Calcium sensitivity of BK-type K_{Ca}, channels determined by a separable domain. *Neuron*. 13, 671–681.

Werner,M.E., P.Zvara, A.L.Meredith, R.W.Aldrich, and M.T.Nelson (2005). Erectile dysfunction in mice lacking the large-conductance calcium-activated potassium (BK) channel. *J. Physiol* 567:545-556.

Williams SE, Wootton P, Mason HS, Bould J, Iles DE, Riccardi D, Peers C, & Kemp PJ (2004). Hemoxygenase-2 is an oxygen sensor for a calcium-sensitive potassium channel. *Science* 306, 2093-2097.

Wood LS & Vogeli G (1997). Mutations and deletions within the S8-S9 interdomain region abolish complementation of N- and C-terminal domains of Ca(2+)-activated K+ (BK) channels. *Biochem Biophys Res Commun* 240, 623-628.

Wu RS, Chudasama N, Zakharov SI, Doshi D, Motoike H, Liu G, Yao Y, Niu X, Deng SX, Landry DW, Karlin A, & Marx SO (2009). Location of the beta 4 transmembrane helices in the BK potassium channel. *J Neurosci* 29:8321-8328.

Wu RS, Liu G, Zakharov SI, Chudasama N, Motoike H, Karlin A, & Marx SO (2013). Positions of beta2 and beta3 subunits in the large-conductance calcium- and voltage-activated BK potassium channel. *J Gen Physiol* 141, 105-117.

Wu,Y., Y.Xiong, S.Wang, H.Yi, H.Li, N.Pan, F.T.Horrigan, Y.Wu, & J.Ding (2009). Intersubunit coupling in the pore of BK channels. *J. Biol. Chem.* 284:23353-23363.

Wu Y, Yang Y, Ye S, & Jiang Y (2010). Structure of the gating ring from the human large-conductance Ca(2+)-gated K(+) channel. *Nature* 466, 393-397.

Xia XM, Ding JP, & Lingle CJ (1999). Molecular basis for the inactivation of Ca2+- and voltage-dependent BK channels in adrenal chromaffin cells and rat insulinoma tumor cells. *J Neurosci* 19, 5255-5264.

Xia XM, Zeng X, & Lingle CJ (2002). Multiple regulatory sites in large-conductance calcium-activated potassium channels. *Nature* 418, 880-884.

Yan J & Aldrich RW (2012). BK potassium channel modulation by leucine-rich repeat-containing proteins. *Proc Natl Acad Sci U S A* 109, 7917-7922.

Yang H, Shi J, Zhang G, Yang J, Delaloye K, & Cui J (2008). Activation of Slo1 BK channels by Mg2+ coordinated between the voltage sensor and RCK1 domains. *Nat Struct Mol Biol* 15, 1152-1159.

Yazejian B, Sun XP, & Grinnell AD (2000). Tracking presynatic Ca2+ dynamics during neurotransmitter release with Ca2+-activated K+ channels. *Nat Neurosci.* 6, 566-571.

Yuan P, Leonetti MD, Pico AR, Hsiung Y, & MacKinnon R (2010). Structure of the Human BK Channel Ca2+-Activation Apparatus at 3.0 A Resolution. *Science*.

Yusifov T, Javaherian AD, Pantazis A, Gandhi CS, & Olcese R (2010). The RCK1 domain of the human BKCa channel transduces Ca2+ binding into structural rearrangements. *J Gen Physiol* 136, 189-202.

Yusifov T, Savalli N, Gandhi CS, Ottolia M, & Olcese R (2008). The RCK2 domain of the human BKCa channel is a calcium sensor. *Proc Natl Acad Sci U S A* 105, 376-381.